

AD-A078 598

FRANKLIN INST RESEARCH LABS PHILADELPHIA PA  
STRESS CORROSION ENVIRONMENTAL EFFECTS ON AF 1410.(U)  
1979 V V DAMIANO

F/G 13/8

UNCLASSIFIED

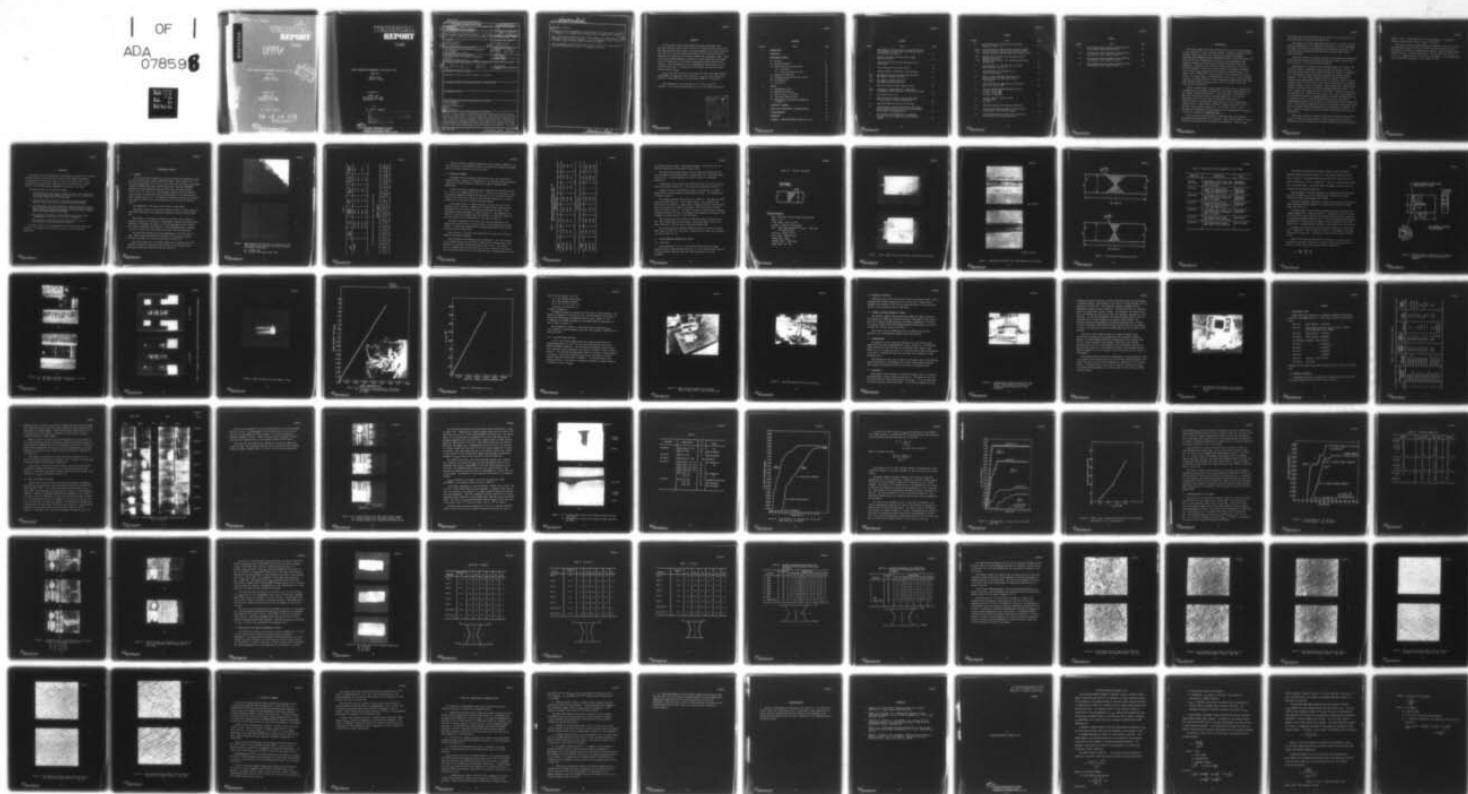
FIRL-F-C4708-01

AFOSR-TR-79-1288

AFOSR-77-3341

NL

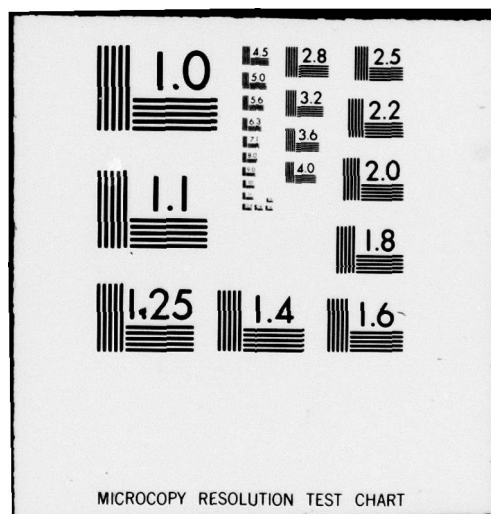
OF  
ADA  
078598



END  
DATE  
FILMED

1-80

DDC





LEVEL

STRESS CORROSION ENVIRONMENTAL EFFECTS ON AF 70H

GRANT NO.

AFOSR-77-3341

NOO NO. 77-3341A

prepared for

AFOSR - FA

# TECHNICAL REPORT

Final Report  
F-C4708-01

STRESS CORROSION ENVIRONMENTAL EFFECTS ON AF 1410

GRANT NO.

AFOSR-77-3341  
MOD NO. 77-3341A

*prepared for*

AFOSR - NA  
Bolling Air Force Base  
Washington, D.C. 20332

*by*

Dr. Victor V. Damiano

AIR FORCE OFFICE OF SCIENTIFIC RESEARCH (AFSC)  
NOTICE OF TRANSMITTAL TO DDC

This technical report has been reviewed and is  
approved for public release IAW AFR 190-12 (7b).  
Distribution is unlimited.

A. D. BLOSE

Technical Information Officer



**Franklin Research Center**

A Division of The Franklin Institute

The Benjamin Franklin Parkway, Phila., Pa. 19103 (215) 448-1000

UNCLASSIFIED

SECURITY CLASSIFICATION OF THIS PAGE (When Data Entered)

19 REPORT DOCUMENTATION PAGE		READ INSTRUCTIONS BEFORE COMPLETING FORM	
1. REPORT NUMBER <b>AFOSR-TR-79-1288</b>	2. GOVT ACCESSION NO.	3. RECIPIENT'S CATALOG NUMBER <b>9</b>	
4. TITLE (and Subtitle) <b>STRESS CORROSION ENVIRONMENTAL EFFECTS ON AF 1410</b>	5. TYPE OF REPORT & PERIOD COVERED <b>FINAL rept.</b> <b>1 May 77 - 30 April 79</b>		6. PERFORMING ORG. REPORT NUMBER
7. AUTHOR(s) <b>VICTOR V. DAMIANO</b>	8. CONTRACT OR GRANT NUMBER(s) <b>AFOSR-77-3341</b>		9. PERFORMING ORGANIZATION NAME AND ADDRESS <b>THE FRANKLIN INSTITUTE RESEARCH LABORATORIES 20th &amp; PARKWAY PHILADELPHIA, PA 19103</b>
10. CONTROLLING OFFICE NAME AND ADDRESS <b>AIR FORCE OFFICE OF SCIENTIFIC RESEARCH/NA BLDG 410 BOLLING AIR FORCE BASE, D C 20332</b>	11. PROGRAM ELEMENT, PROJECT, TASK AREA & WORK UNIT NUMBERS <b>2307B2</b> <b>61102F</b>		12. REPORT DATE <b>11 1979</b>
13. MONITORING AGENCY NAME & ADDRESS (if different from Controlling Office) <b>FIRL-F-04798-01</b>	14. SECURITY CLASS. (of this report) <b>UNCLASSIFIED</b>		15. DECLASSIFICATION/DOWNGRADING SCHEDULE
16. DISTRIBUTION STATEMENT (of this Report) <b>Approved for public release; distribution unlimited.</b>			
17. DISTRIBUTION STATEMENT (of the abstract entered in Block 20, if different from Report)			
18. SUPPLEMENTARY NOTES			
19. KEY WORDS (Continue on reverse side if necessary and identify by block number) <b>STRESS CORROSION AF 1410 PLATES MECHANICAL PROPERTIES WELDED CRACK EXTENSION</b>			
20. ABSTRACT (Continue on reverse side if necessary and identify by block number) <b>AF 1410 plates available from Universal Cyclops through Air Force Materials Laboratory under contract F33615-73-C-5093 were welded using filler wire fabricated from sheet stock of the same composition as the base plate and from 1/16" Dia. weld wire prepared by Universal Cyclop from AF-1410 stock. The method of welding was cold wire-gas tungsten arc using manual feed. Satisfactory welds having mechanical properties as welded approaching the properties of the base plate in the double austenitized and aged condition were obtained. SCC tests</b>			

DD FORM 1 JAN 73 1473

UNCLASSIFIED

SECURITY CLASSIFICATION OF THIS PAGE (When Data Entered)



Unclassified

SECURITY CLASSIFICATION OF THIS PAGE (When Data Entered)

Block 20. Abstract.

demonstrated that nonhomogeneous microstructures in the fusion zone may result in nonuniform crack extension and seriously affect estimates made of  $K_{ISCC}$ .

$K_{ISCC}$  values were obtained for base plate and welds using wedge opening loading (WOL) and cantilever beam techniques.  $K_{ISCC}$  for base plate varied from 28 to 30 ksi $\sqrt{in}$ , values for welds varied from 22 to 48 ksi $\sqrt{in}$ .

Crack propagation rates increased from  $2 \times 10^{-4}$  to  $50 \times 10^{-4}$  inches/hr with increased loading from  $K_{10} = 30$  to 60 ksi $\sqrt{in}$  respectively.

Unclassified

SECURITY CLASSIFICATION OF THIS PAGE (When Data Entered)

## ABSTRACT

AF 1410 plates available from Universal Cyclops through Air Force Materials Laboratory under contract F33615-73-C-5093 were welded using filler wire fabricated from sheet stock of the same composition as the base plate and from 1/16" Dia. weld wire prepared by Universal Cyclop from AF-1410 stock. The method of welding was cold wire-gas tungsten arc using manual feed. Satisfactory welds having mechanical properties as welded approaching the properties of the base plate in the double austenitized and aged condition were obtained. SCC tests demonstrate that nonhomogeneous microstructures in the fusion zone may result in nonuniform crack extension and seriously affect estimates made of  $K_{ISCC}$ .

$K_{ISCC}$  values were obtained for base plate and welds using wedge opening loading (WOL) and cantilever beam techniques.  $K_{ISCC}$  for base plate varied from 28 to 30 ksi $\sqrt{\text{in}}$ , values for welds varied from 22 to 48 ksi $\sqrt{\text{in}}$ .

Crack propagation rates increased from  $2 \times 10^{-4}$  to  $50 \times 10^{-4}$  inches/hr. with increased loading from  $K_{10} = 30$  to 60 ksi $\sqrt{\text{in}}$  respectively.

Accession For	
NTIS GRA&I	<input checked="checked" type="checkbox"/>
DDC TAB	<input type="checkbox"/>
Unannounced	<input type="checkbox"/>
Justification	
By	
Distribution/	
Availability Codes	
Dist	Avail and/or special
A	



## CONTENTS

Section	Title	Page
1	INTRODUCTION . . . . .	1
2	OBJECTIVES . . . . .	4
3	EXPERIMENTAL METHODS . . . . .	5
	3.1 Material . . . . .	5
	3.2 Welding Procedures . . . . .	8
	3.3 Stress Corrosion Cracking Tests . . . . .	10
	3.3.1 WOL Tests. . . . .	10
	3.3.2 Cantilever Beam SCC Tests . . . . .	23
	3.4 Mechanical Properties. . . . .	26
	3.5 Scanning Electron Microscopic Studies . . . . .	26
	3.6 Cinematography . . . . .	26
	3.7 Ultrasonics . . . . .	26
4	RESULTS . . . . .	30
	4.1 Radiographic Tests . . . . .	30
	4.2 Mechanical Properties. . . . .	30
	4.3 WOL SCC Tests in 3.5% NaCl. . . . .	32
	4.4 Cantilever Beam SCC Tests . . . . .	43
	4.5 Metallurgical and Chemical Homogeneity of Welds . . . . .	48
5	DISCUSSION & SUMMARY . . . . .	62
6	STATUS AND SIGNIFICANCE OF RESEARCH EFFORT . . . . .	64
	ACKNOWLEDGEMENTS . . . . .	67
	REFERENCES . . . . .	68
	APPENDIX I FRACTURE MECHANICS APPROACH TO SCC. . . . .	69

## FIGURES

Number	Title	Page
1	Metallographic Cross Sections of As-Received AF-1410 Sheet Showing the Oxide Layer (Top) and the Overall Cleanliness of the Steel . . . . .	6
2	Special Copper Back Up Plate Used to Purge Back Side of Weld . . . . .	12
3	Completed Weld Using AF-1410 Sheet Material as Filler Wire . . . . .	13
4	Joint Design AF-1410-2 and AF-1410-3. . . . .	14
5	Detailed Drawing of Modified 1-T WOL Specimen . . . . .	17
6(a)	WOL Samples from Weld and Base Plate AF-1410-2	
(b)	WOL Samples from Weld AF-1410-3 . . . . .	18
7(a)	WOL Samples from Weld AF-1410-5	
(b)	WOL Samples from Weld AF-1410-6 . . . . .	19
8	NASA Clip Gage with Strain Gages in Place. . . . .	20
9(a)	Calibration of Gage Opening vs. Gage Output	
(b)	Arrangement of Microscope Used to Calibrate Clip Gage. . . . .	21
10	Correlation of $K_I$ to $V_o$ . . . . .	22
11	NASA Clip Gage Arranged on WOL Specimen Ready for Application of Load by Torquing Bolt . . . . .	24
12	Cantilever Beam Test Ring for SCC Testing. . . . .	25
13	Cinematographic Apparatus Showing Dual 16mm Cameras WOL Specimen and Corrosion Cell for the Continuous Monitoring of Crack Propagation . . . . .	27
14	WOL Specimens with Transducer for Ultrasonic Evaluation of Crack Growth and the Krautkramer System . . . . .	29



## FIGURES

Number	Title	Page
15	Crack Propagation in AF-1410-2 Weld and Base Plate $K_{I0} = 40$ ksi in. . . . .	33
16(a)	Fracture Surface of AF-1410-2 Weld Tested by MetCut	
(b)	Fracture Surface of AF-1410-2 Weld Tested by FIRL	
(c)	Fracture Surface of AF-1410 Base Plate Tested by FIRL . . . . .	35
17(a)	Enlarged View of Figure 14(b) Showing Irregular Fatigue Crack Front	
(b)	Enlarged View of Figure 14(c) Showing Fatigue Crack and Sec Crack . . . . .	37
18	Crack Extension vs. Time WOL Test of AF-1410 Base Plate $K_{I0} = 40$ ksi in. . . . .	39
19	Crack Extension vs. Time WOL Test of AF-1410-5 Base Plate . . . . .	41
20	Effect of $K_{I0}$ on Average Crack Velocity of AF-1410-5 Base Plate Aged (950° F-4hrs.) from Figure 19 . . . . .	42
21	Crack Extension vs. Time WOL Test of AF-1410-5 Weld. $K_{I0} = 30$ ksi $\sqrt{\text{in.}}$ . . . . .	44
22	Fractured Surface of WOL Specimens AF-1410-6 (a) $K_{I0} = 30$ ksi $\sqrt{\text{in.}}$ (b) $K_{I0} = 40$ ksi $\sqrt{\text{in.}}$ (c) $K_{I0} = 45$ ksi $\sqrt{\text{in.}}$ . . . . .	46
23	Fracture Surface of AF-1410-5 WOL (a) Base Plate (b) Weld . . . . .	47
24	Weld Cross Sections with Hardness Impressions . . . . .	49
25	Back Scattered Electron Image of Weld AF-1410-2 at Positions 1 and 2 Shown in Table V . . . . .	56
26	Back Scattered Electron Image of Weld AF-1410-2 at Positions 3 and 4 Shown in Table V . . . . .	57



## FIGURES

Number	Title	Page
27	Back Scattered Electron Image of Weld AF-1410-2 at Positions 5 and 8 Shown in Table V . . .	58
28	Back Scattered Electron Images of Weld AF-1410-3 at Positions 1 and 2 Shown in Table VI . . .	59
29	Back Scattered Electron Images of Weld AF-1410-3 at Positions 3 and 4 Shown in Table VI . . .	60
30	Back Scattered Electron Images of Weld AF-1410-3 at Positions 5 and 6 Shown in Table VI . . .	61

## 1. INTRODUCTION

Most high strength steels have characteristically low fracture toughness and low resistance to stress corrosion cracking. Through a cooperative effort by United States Steel (USS) and the Naval Ship Research Development Laboratory under NAVSHIPS Contract NObs-88540 and 94535 a 10Ni-2Cr-1Mo-8Co-.11C Steel (Hy-180) was developed which provided the best compromise of high strength, toughness, excellent stress corrosion cracking resistance and weldability. Extensive stress corrosion cracking evaluation of a family of Hy-180/210 candidate alloys led to the selection of an optimum alloy composition in which  $K_{ISCC}$  values of both the plates and weld metal were in the range of 130 to 150 ksi $\sqrt{\text{in.}}$ . Minor alterations in the composition and purity resulted in a higher degree of susceptibility of the alloy to stress corrosion cracking. Air melted base metal and gas tungsten arc (GTA) welded 12N-5Cr-3Mo steel systems resulted in  $K_{ISCC}$  values of 44 to 33 ksi $\sqrt{\text{in.}}$  for the base plate and weld respectively.

Hy-180, although having a high strength and high fracture toughness, was not competitive on a weight-to-strength basis with other candidate materials for aircraft structural application. A new alloy AF1410 (14Co-10Ni-2Cr-1Mo-0.16C) was developed jointly by General Dynamics and U.S. Steel by sponsorship of the Air Force Materials Laboratory under contract F33615-73-C-5093. The mechanical property goals set in this program were ultimate tensile strength (UTS) of 230/280 k, tensile yield (TY) of 220 ksi and plane strain fracture toughness  $K_{Ic}$  115 ksi $\sqrt{\text{in.}}$ . Details of the rationale and experimental work associated with the development and evaluation of AF1410 are summarized in AFML-TR-75-148. A 021174

Pilot plant production quantities of 2000 pound heats were produced exhibiting the desired mechanical properties. Only a limited number of stress corrosion cracking tests were conducted on the baseplate. Values of  $K_{ISCC}$



100 ksi $\sqrt{\text{in.}}$  were initially reported but the results were questionable due to crack branching and deviation from ASTM 399-70.

The potential for large scale usage of AF 1410 as a structural aircraft material, demonstrated in the AFML-TR-75-148 project, led to the development of commercial practices for the manufacture of production quantities of AF 1410 by Universal Cyclops Specialty Steel Division under AFML contract F33615-76-C-5026.

Recent data reported by Universal Cyclops on the mechanical properties of their production quantities indicates that the goal of UTS = 230/250, TYS = 220 ksi and  $K_{Ic} = 120 \text{ ksi} \sqrt{\text{in.}}$  had been achieved.

The weldability of AF-1410 by cold wire-gas tungsten arc (CW-GTA), hot wire gas tungsten arc (HW-GTA) and electron beam weld processes was also investigated under AFML Contract F33613-73-C-5013 and reported in AFML-TR-75-148. All welding in these studies was performed with automatic welding equipment. The filler metal composition used for CW-GTA and HW-GTA in accordance with studies made on 10Ni-Cr-Mo-Co (by USS) was close in the major alloying elements to AF-1410 base plate, with the exception of the residual elements aluminum, silicon and vanadium. These elements were increased above the level of the base plate to achieve an optimum deoxidation effect. The sulfur, oxygen, and nitrogen were held to low levels in the weld wire and in the deposited weld. Carbon was held to about 0.1%. The welding parameters for the CW-GTA processes for optimum properties included low energy input and low deposition rates. The manual CW-GTA process was not investigated, although manual processes are conducive to low energy input and low deposition rates. The mechanical properties achieved by the automatic CW-GTA process did meet the minimum strength requirements after post aging heat treatment. No  $K_{ISCC}$  testing to evaluate the stress corrosion cracking sensitivity of welds was conducted.

Recent data obtained by Rockwell International indicates that values of  $K_{ISCC}$  for Universal Cyclops prepared AF-1410 base plate of 30 ksi $\sqrt{\text{in.}}$  in 3.5% NaCl solution are typical for the double austenitized and aged condition

(950°F - 5 hrs.). Welds made with weld wire prepared by U.S. Welding in Tarzana, California gave values of  $K_{ISCC} = 60 \text{ ksi} \sqrt{\text{in.}}$

The present research program supported by AFOSR under contract 77-3341 is concerned with the study of stress corrosion cracking of welded AF 1410 in both aqueous and gaseous environments using material supplied by AFML through Universal Cyclops. The grant issued May 1, 1977 was under the direction of Dr. Victor V. Damiano who was the principal investigator. The following final report covers the period May 1, 1977 to April 30, 1979.

## 2. OBJECTIVES

The objective of the program was to investigate the sensitivity of welded AF-1410 plates to stress corrosion cracking in both aqueous and gaseous environments and to study the nature of subcritical growth crack in welds including crack growth rates, crack path and the interrelation of these factors to the solidification inhomogeneities arising in the welds.

The specific goals of the program included:

1. The preparation of welds using a manual cold wire - gas tungsten arc technique (CW-GTA) and commercially available AF-1410 and weld wire of the same composition as the base plate.
2. The evaluation of the quality of the welds using radiographic analysis, scanning electron microscopy and mechanical tests.
3. The evaluation of the stress corrosion cracking sensitivity of the welds using plane strain conditions and a fracture mechanics approach in both aqueous and gaseous environment, with wedge opening loading (WOL) and cantilever Beam (CB) specimens.
4. The study of the subcritical crack growth rates and path using cinematographic recording of in situ crack propagation.
5. The correlation of subcritical crack growth behavior to the solidification structures produced by welding.

The final results of this program may have practical significance with respect to the feasibility of field weld repairs of AF-1410 aircraft structures.



### 3. EXPERIMENTAL METHODS

#### 3.1 MATERIAL

AF-1410 plates were furnished by Universal Cyclops with permission of the Air Force Officer under contract F33615-76-C-5026. Twenty plates of 4" x 8" x 5/8" and twenty plates of 4" x 8" x 1" were received in the double austenitized condition (1650°F/30 min./WQ + 1500°F/30 min./W.Q.) from heat #L3550K19. Details of the melting and fabrication of this heat are given in Report IR-160-6 (I), (II), and (III). Metallographic studies of the "As Received" plates revealed a surface scale and low concentration of included oxides as seen in Figure 1(a) and (b). The mechanical properties reported for this heat after aging at 950°F 5 hrs./AC and processing to 1.25" plate are given in Table I.

The composition of this heat stirred ingot is given below.

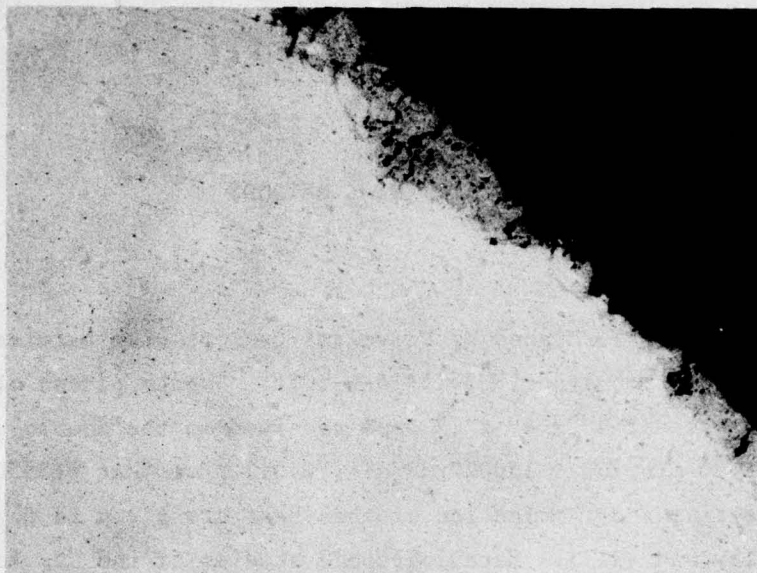
Preliminary studies in welding were conducted using 1/16" wide strips cut from 0.062" thick sheet stock supplied by Universal Cyclops from heat #3616 K13.

The surfaces of the sheets, which had a mill scale, were cleaned by mechanical abrasion of the surface. Metallographic samples were prepared from each sheet to determine the extent of the oxide penetration and to evaluate the overall cleanliness of the material. The micrographs shown in Figures 1(a) and (b) reveal the surface oxide scale and a fine oxide dispersion.

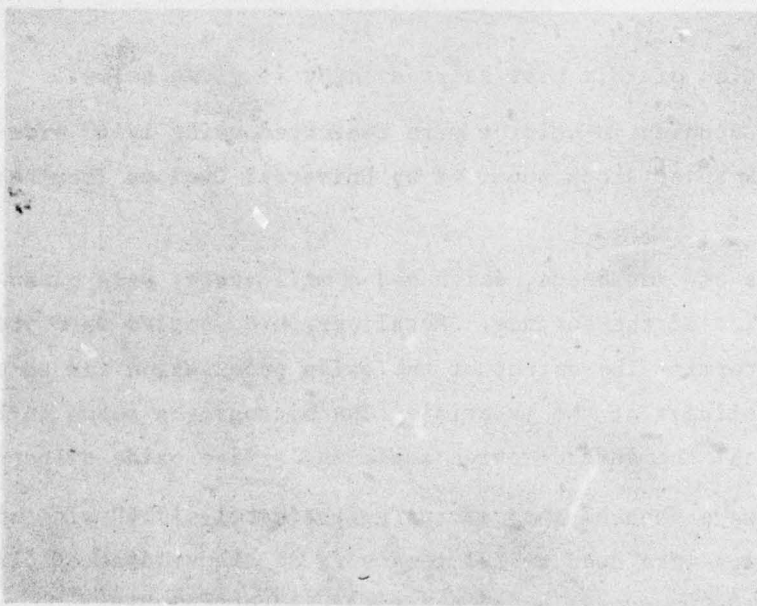
The sheets were sheared into strips approximately 1/16" wide and 13" long. These strips were used as the feed wire in the welding of plates AF-1410-1, AF-1410-2, and AF-1410-3 described in section 3.2.

Weld wire (0.062" dia. of the same composition as the base plate also prepared by Universal Cyclops was received later in the program and all additional welding was conducted using this weld wire.

C4708-01



A



B

Figure 1. Metallographic Cross Sections of As-Received AF 1410 Sheet Showing the Oxide Layer (Top) and the Overall Cleanliness of the Steel.

- A) - Surface Scale
- B) - Internal Cross Section Mag. 150X



Table I.

HEAT	TEST DIRECT	UTS ksi	YIELD STRENGTH ksi	ELONG. %	RED. IN AREA	CVN R.T. FT. LBS.	HARDNESS R <sub>C</sub>
L3550K19	L	246.5	226.6	17.2	72.9	71.5	48.1
	L	248.8	231.2	15.6	71.5	68.0	
	T	255.9	234.2	15.2	68.5	61.0	48.2
	T	254.2	233.8	15.9	71.2	69.0	

The composition of this heat stirred ingot is given below.

## ELEMENT PERCENT

C	Mn	Si	S	P	Cr	Ni	Co	Mo	Al	Ti	N	O	Fe
0.17	0.06	0.03	0.002	0.004	2.05	10.19	14.01	1.04	0.001	0.004	0.001	0.0002	Bal.



Weld wire having an adjusted composition in the residual elements Al, Si and vanadium was not available so that all the welds were prepared using weld wire of the same composition as the base plate.

### 3.2 WELDING PROCEDURES

Procedures for GTA welding of 10Ni-Cr-Mo-Co steel were described in Technical Report, Project No. 33018-007(51) by The Applied Research Laboratory (USS) and for 14Co-10Ni-1Mo-0.1C (AF-1410) by General Dynamics Report ERR-FW-1565.

In those studies, an attempt was made to maintain the residuals (Mn, Si, Al, V, and Ti) at minimum levels and S, P, O, and N at very low levels. Both of the above references indicate that additions of 0.10 to 0.20% Si and up to 0.02% Al and 0.10% V were required in the weld wire composition to prevent porosity in the welds and to achieve optimum toughness.

In the present work, no attempt was made to adjust the level of the residuals of the weld wire. Commercially available sheet stock having the same composition as the base plate from heat L3616-K13 and used in the preliminary welding experiments is shown in Table II. The composition of 0.062" dia. weld wire prepared from heat L3616-K14 by Universal Cyclops and used for welding in later experiments is also shown in Table II.

The major differences in the 0.062" dia. weld wire and sheet stock composition previously used as filler rod were in the aluminum and nitrogen content. The weld wire contained more aluminum and nitrogen than both the base plate and the sheet stock.

The weld wire, as received, was covered with an oxide scale which was removed by mechanical abrasion.

Since acceptable weld parameters were established in the prior studies for the CW-GTA process, and the process lends itself to manual feed, it was selected as the method of welding for the present studies. The CW-GTA process, although very slow and inefficient, is well suited for the present study since high quality welds can be prepared with a minimum tendency to pick

Table II. Chemical Analyses of Weld Wire, L3616-K14  
Base Plate, and L3616-K13 Sheet Stock  
Element Percent

SAMPLE	C	Mn	P	S	Si	Ni	Cr
Weld Wire	0.175	0.13	0.005	0.002	0.01	9.87	2.07
L3616-K14	0.16	0.09	0.003	0.001	0.04	10.00	0.94
L3616-K13	0.16	0.13	0.005	0.002	0.03	10.0	2.07

Element Percent

SAMPLE	Mo	Ti	Co	Al	V	N	O
Weld Wire	0.87	0.005	13.1	0.010	0	0.048	0.002
L3616-K14	0.96	0.004	13.98	0.003	0	0.0004	0.0015
L3616-K13	0.95	0.005	13.95	0.002	0	0.007	0.0011

up residuals such as oxygen, nitrogen and hydrogen. The process also has practical application in the field for weld repair.

The welding was performed using a 300 amp Linde UCC 305 machine, with foot attachment for amperage control in conjunction with a Linde HW-20 water cooled torch. A contact pyrometer was used to monitor the interpass temperature.

A preliminary test weld was run utilizing the 5/8" thick plates and the joint design shown in Table III. This plate was designated as AF-1410-1.

A special back-up fixture shown in Figure 2 was used for all manual CW-GTA welds to provide auxiliary back-up gas shielding. The completed weld is shown in Figure 3.

The welding parameters used are given in Table III. Two additional weld joints were made using the 1" thick plates after it was determined that AF-1410-1 was satisfactory. These plates, designated AF-1410-2 and AF-1410-3, were welded along the 8" edge of the plates. The joint design for these plates is shown in Figure 4. The double V design was selected for the Stress Corrosion Cracking test since it presented a more symmetrical design for crack propagation studies parallel to the weld beads.

The included angle for AF-1410-2 was 90° while that for AF-1410-3 was 60°. The included angle was decreased to reduce the amount of the filler metal required for the weld and to reduce the welding time.

All subsequent welds including assemblies AF-1410-4 to AF-1410-10 were made using the 0.062" dia. weld wire. A description of these weld assemblies is given in Table IV. 3.3

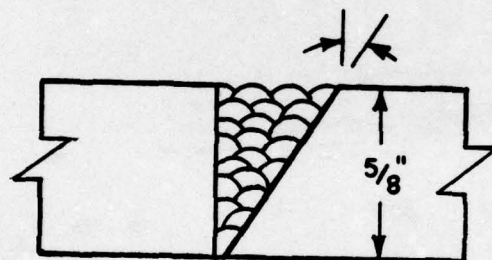
### 3.3 STRESS CORROSION CRACKING (SCC) TESTS

#### 3.3.1 WOL Tests

Plates measuring 8" x 4" x 1" which were welded along the 8" edge provided 2 WOL 1-T SCC specimens while 8" x 4" x 5/8" plates welded along the 8" edge provided 4 WOL base plate and 3 WOL fusion zone 1/2 -T SCC specimens.



Table III. AF-1410-1 Test Weld

PRELIMINARY  
JOINT DESIGNWelding Parameters

Amps - Root Pass 120-130, Filler Passes 130-140

Volts - 12-13

Travel Speed - Avg. 2.75 IPM

Tungsten - 3/32 Dia. 2% thoriated

Wire - .080" sheet sheared into strips .080" wide  
or 0.062 dia wire

Torch gas - Argon @ 15 CFh

Back up gas - Argon @ 5 CFh

Preheat Temp - None

Interpass Temp. - 200°F Max.

Energy Input - 31.2 KJ

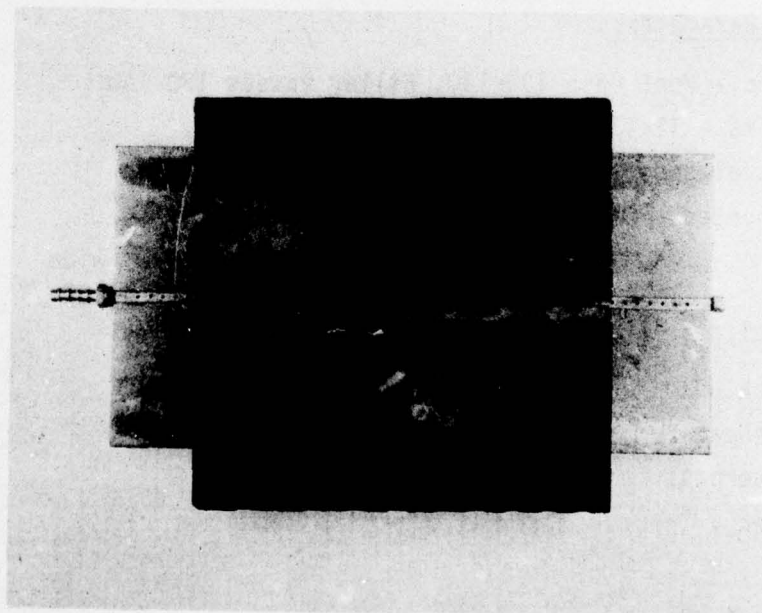
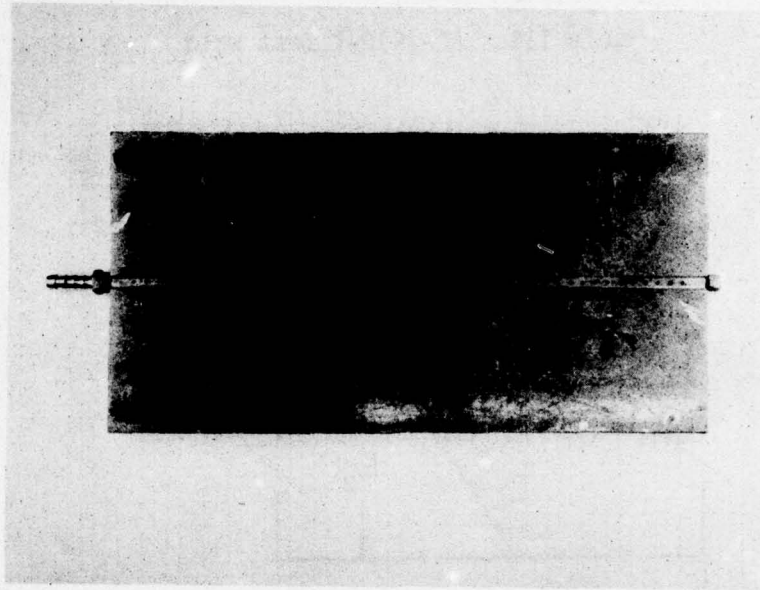
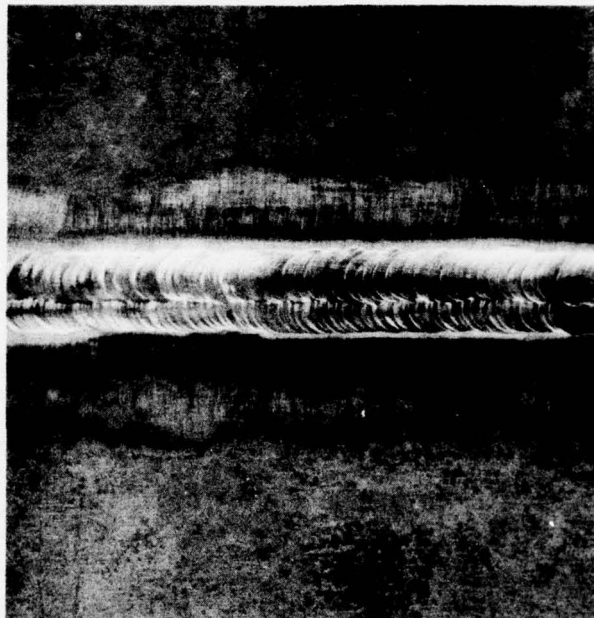
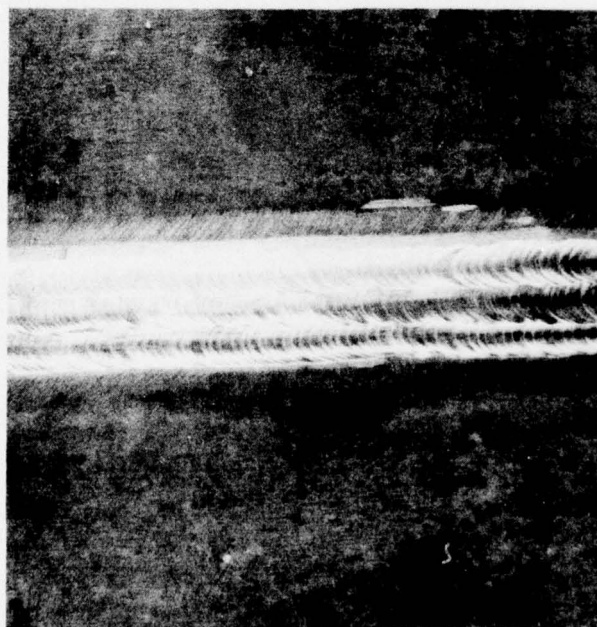


Figure 2. Special Copper Back Up Plate Used to Purge Back Side of Weld

C4708-01



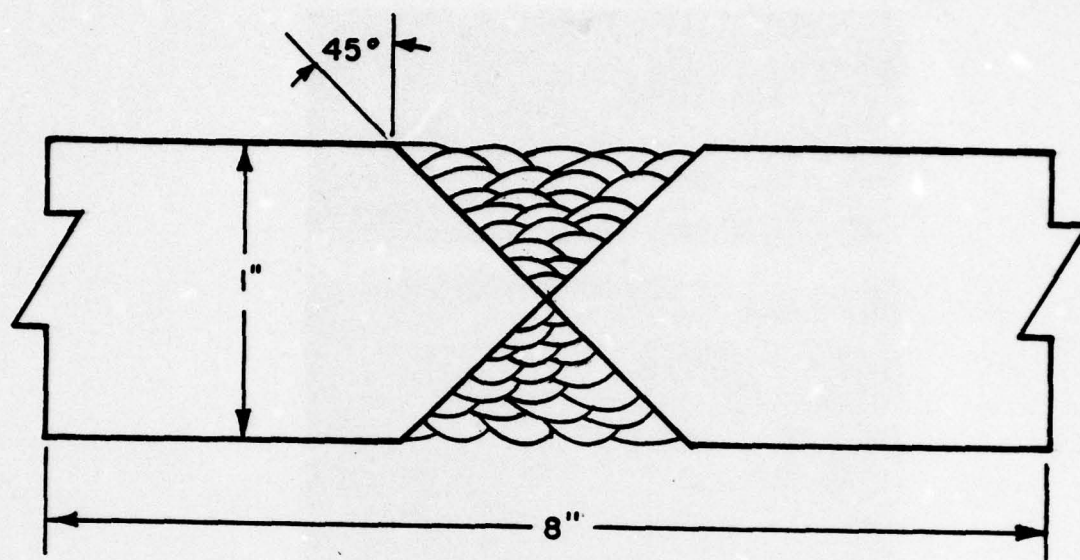
Top of Weld A



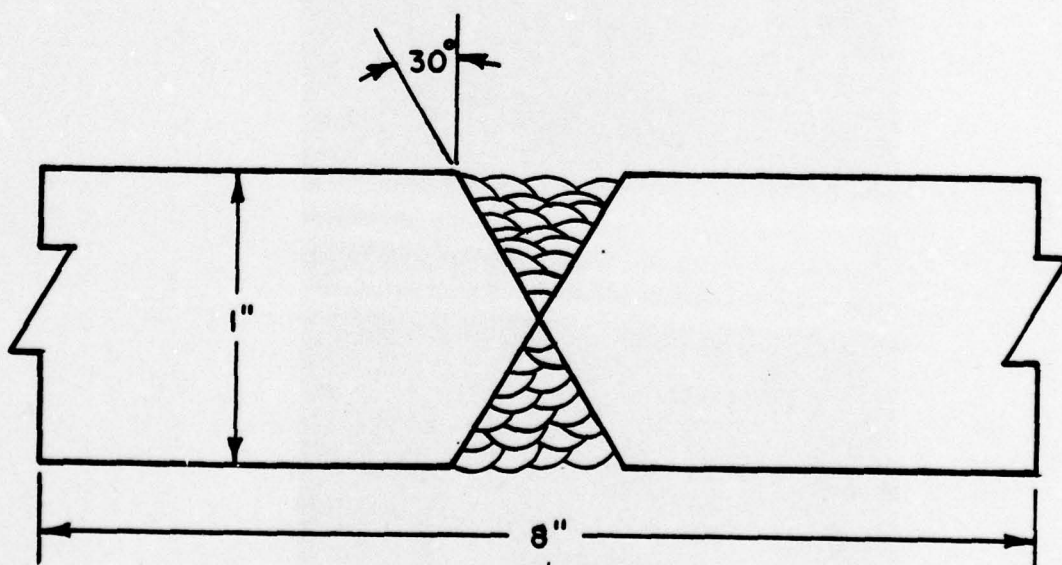
Bottom of Weld B

Figure 3. Completed Weld Using AF 1410 Sheet Material as Filler Wire





AF-1410-2



AF-1410-3

Figure 4. Joint Design AF-1410-2 and AF-1410-3

Table IV. Description of Weld Assemblies of 5/8" Plates

SAMPLE NO.	DESCRIPTION	TESTS
AF-1410 Test Plate	CW-GTA Weld along 8" edge. Pre-aged (950°F- 4 hrs) then welded tests "as welded"	Mechanical Radiographic
AF-1410-5	CW-GTA Weld along 8" edge. Welded in austenitized condition - then aged (950°F-4 hrs)	Mechanical Radiographic (WOL) SCC
AF-1410-6	CW-GTA Weld along 8" edge. Pre-aged (950°C-4 hrs) then welded tests "as welded".	Mechanical Radiographic (WOL) SCC
AF-1410-7	CW-GTA Weld along 4" edge. Welded in austenitized condition - then aged (950°F-4 hrs)	Radiographic (CLB) SCC
AF-1410-8	CW-GTA Weld along 4" edge. Pre-aged (950°F-4 hrs) then welded tests "as welded"	Radiographic (CLB) SCC
AF-1410-9	CW-GTA Weld along 8" edge. Aged (950°F-4 hrs) then welded	Radiographic
AF-1410-10	CW-GTA Weld along 4" edge. Aged (950°F-4 hrs) then welded	Not Evaluated



The samples were machined and fatigue cracked by Met Cut Research Associates following Novak and Rolfe's (2) modified WOL specimen design as shown in Figure 5. WOL samples machined from AF-1410-2 and AF-1410-3 are shown in Figures 6(a) and (b) respectively. Figure 6(a) shows one base plate and one weld WOL sample. The second (WOL) weld sample from this plate was tested by Met Cut Research Associates.

The arrangement of WOL test specimens cut from AF-1410-5 and AF-1410-6 are shown in Figures 7(a) and (b) respectively. Mechanical tests were conducted from the remaining material as shown.

The NASA displacement gage shown in Figure 8 was constructed according to ASTM designation E399-70T, Appendix A, following details given by Fisher, Bubsey and Srawley (3).

The gage consists of two cantilever beams and a spacer block which are clamped together with a single nut and bolt. The material used for the gage was 13V-11Cr-3Al titanium alloy in the solution treated condition because of its high yield strength to modulus ratio. Four 120 strain gages were mounted longitudinally on each side of the beams as close as possible to the beam-spacer block. The gage bonding conformed to the manufacturer's specification.

The gage was calibrated using the calibrated eyepiece of a light microscope - Figure 9(b). The mv output/volt input vs. displacement of the gage are plotted in Figure 9(a). The gage was linear over the range of 0.200 to 0.250".

Nominal crack opening displacements  $V_o$  required to initially load 1-T modified WOL specimens of AF-1410 to a given  $P$  of  $K_{I0}$  value are plotted in Figure 10. These data were generated from the relationship

$$V_o = \frac{K_{I0}}{E} \times \frac{A_o B}{B} \frac{C_6}{C_3}$$

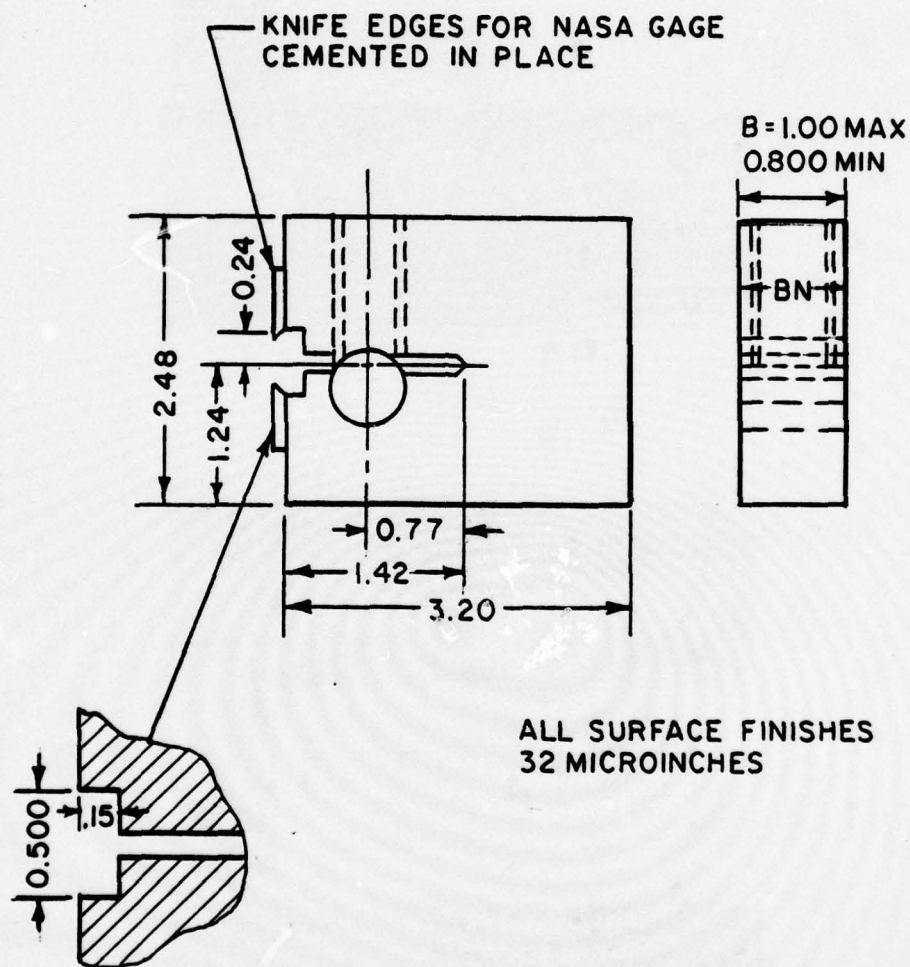


Figure 5. Detailed Drawing of Modified 1/T WOL Specimen  
Dimensions One Half Those Shown for 1/2-T  
Specimens

APR 17 1965  
JAMIANO

C4708-01

AF1410-2

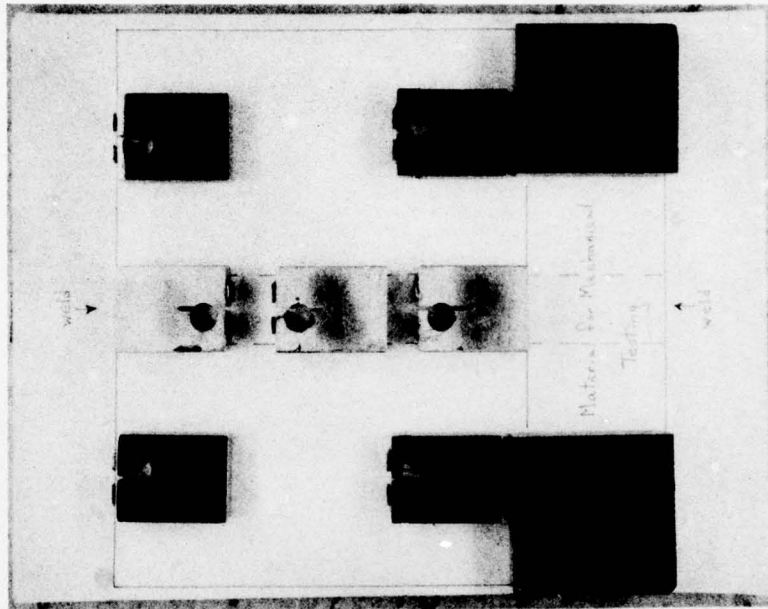
(a)

AF1410-3

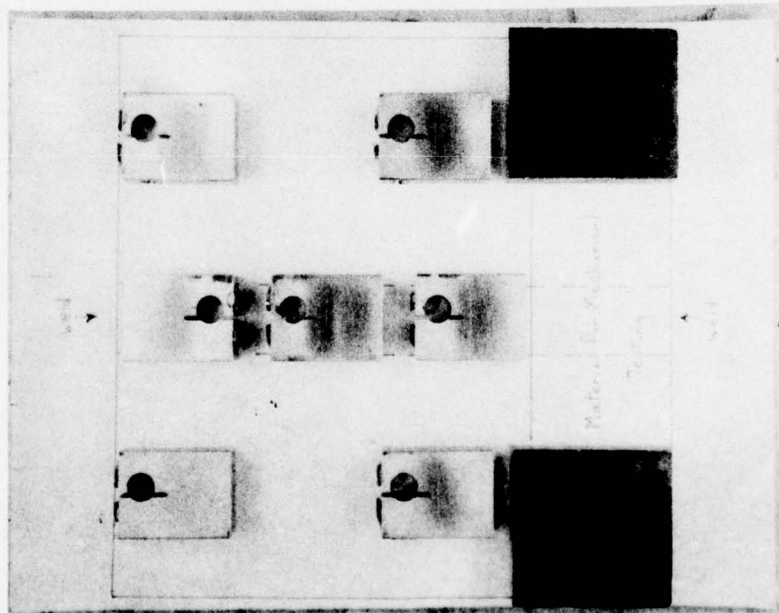
(b)

Figure 6. (a) - WOL Samples from Weld and Base Plate - AF-1410-2  
(b) - WOL Sample from Weld AF-1410-3





b. AF-1410-6



a. AF-1410-5

Figure 7. Arrangement of WOL Test Specimens Cut from AF-1410-5 and AF-1410-6 Weld Assemblies

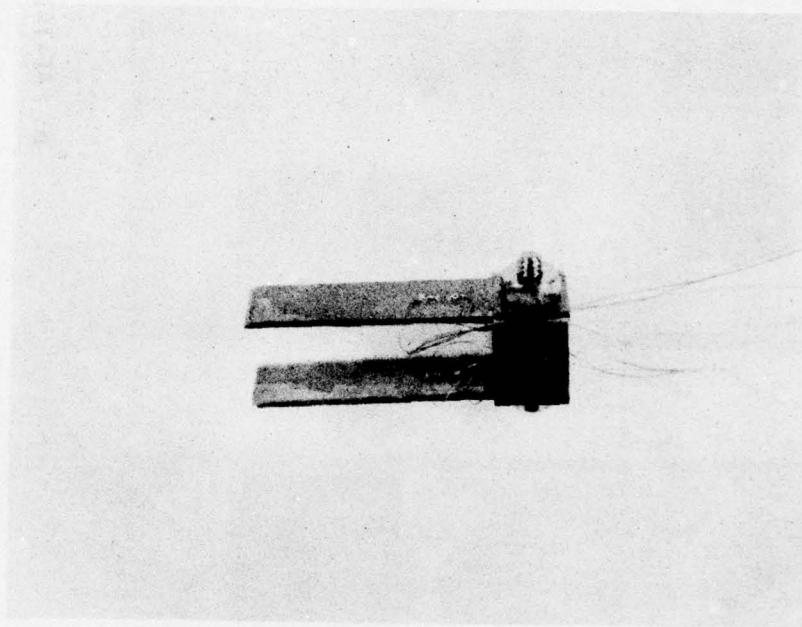


Figure 8. NASA Clip Gage with Strain Gages in Place

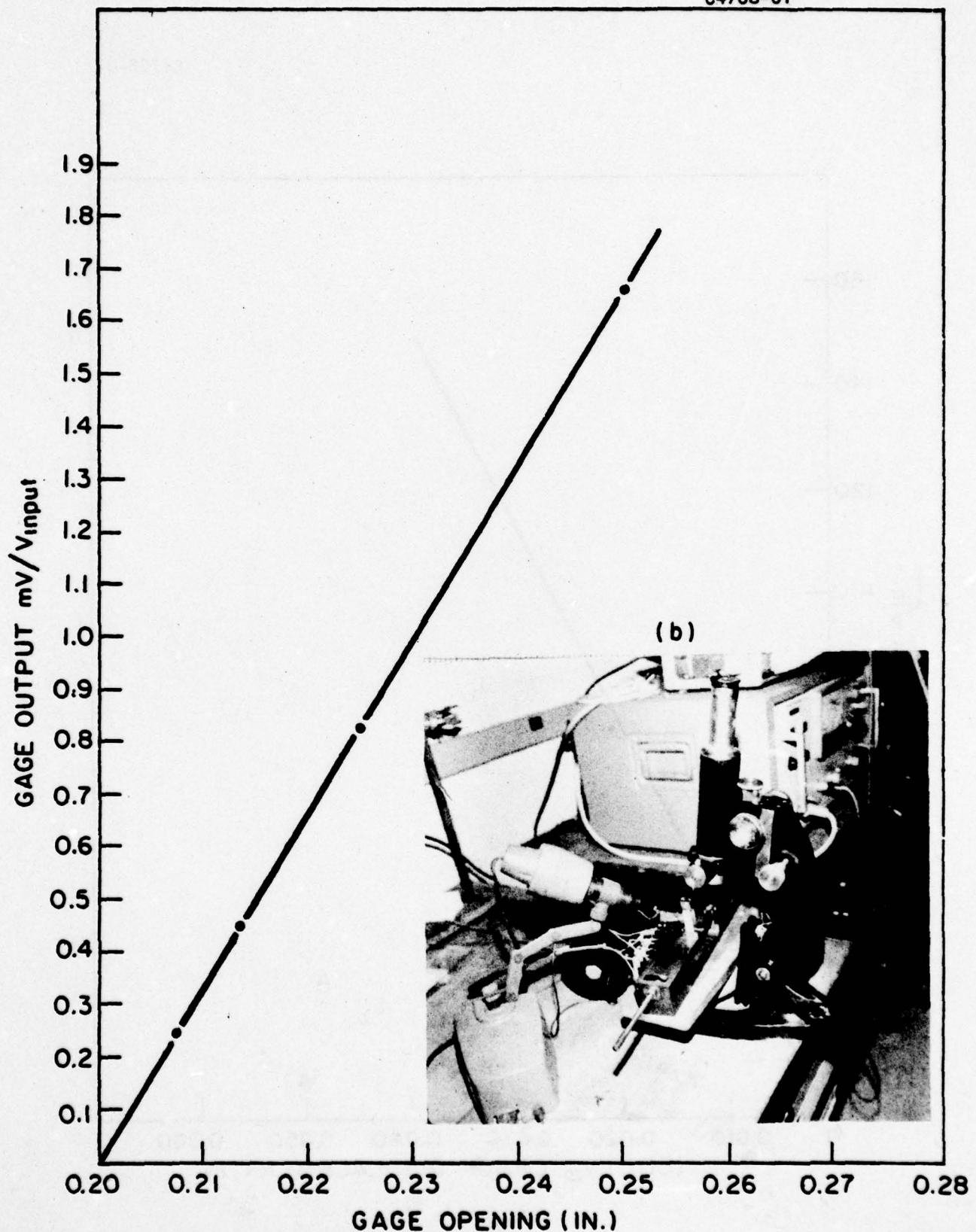


Figure 9. (a) Calibration of Gage Opening vs. Gage Output  
(b) Arrangement of Microscope Used to Calibrate Clip Gage.



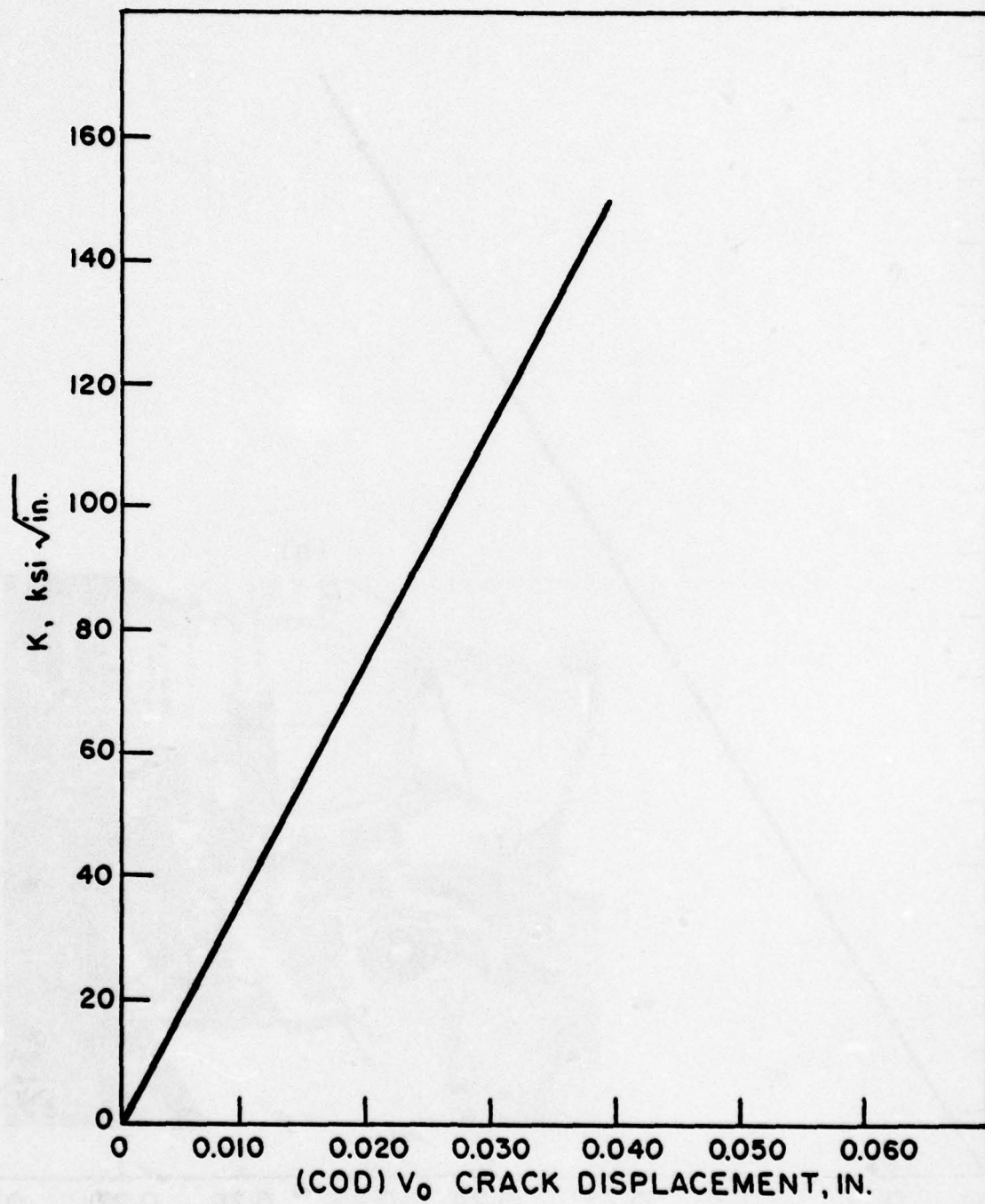


Figure 10. Correlation of  $K_I$  to  $V_0$

where  $E$  is the modulus =  $28 \times 10^6$

$A_0$  is the original crack length

$B_n$  is the specimen thickness

$B = 1"$  for 1-T,  $0.5"$  for 1/2-T

$C_6$  and  $C_3$  are a function of  
as given in Appendix 1.

The NASA clip gage was inserted into the clips of the WOL specimen. The sample was gripped in a vise and the bolt, after lubrication, was torqued to provide the desired  $K_{I0}$  as determined from the graph, Figure 10. The arrangement of the NASA clip gage on the specimen ready for application of load is shown in Figure 11.

WOL specimens are loaded to a given  $K_{I0}$  above the suspected  $K_{ISCC}$  value immersed in the environment of test and crack movement is monitored on a continuous basis.

### 3.3.2 Cantilever Beam SCC Tests

4" x 8" x 5/8" plates welded along the 4" edge provided three test specimens measuring 1" x 1/2" x 16" for cantilever beam SCC tests by the method developed by Brown (4). The pre-notched and fatigue cracked bar was held horizontally and surrounded at the notch by 3.5% NaCl in water as seen in Figure 12. The specimen was dead-weight loaded for periods of time extending to 500 hours. The stress intensity factor  $K_{\sigma}$  was calculated for various loading conditions as described in Appendix 1. By incorporating a step loading procedure it was possible to minimize the number of samples required to establish a value of  $K_{ISCC}$ .



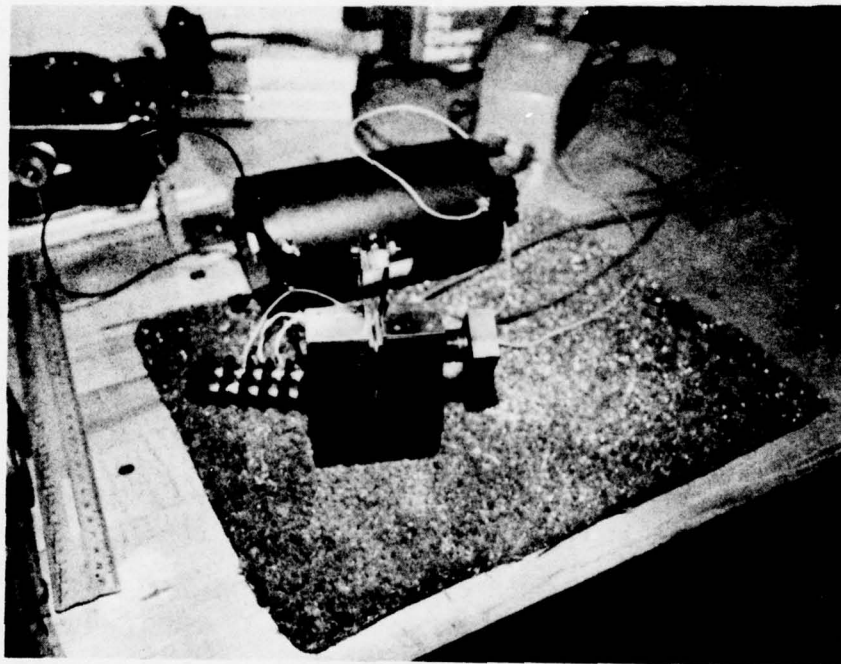


Figure 11. NASA Clip Gage Arranged on WOL Specimen  
Ready for Application of Load by Torquing Bolt

C4708-01

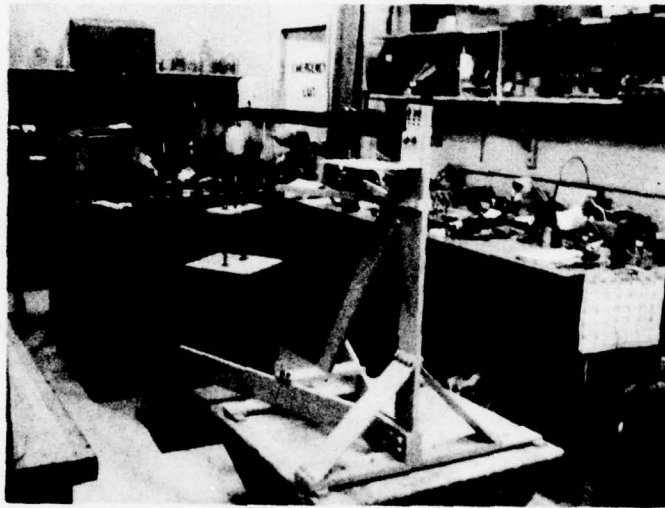


Figure 12. Cantilever Beam Test Ring for SCC Testing

### 3.4 MECHANICAL PROPERTIES

Mechanical tests of the weld included tensile and charpy V-notch. These specimens were machined perpendicular to the weld joint. Charpy V-notch specimens were notched so that the crack path was parallel to the weld bead, similar to the orientation used for SCC tests.

### 3.5 SCANNING ELECTRON MICROSCOPIC STUDIES

The JSM-50A scanning electron microscope (SEM) with energy dispersive X-ray capability (EDXA) and a Northern Scientific 880 computer based system was used to analyze the metallurgical and chemical homogeneity of the welds. For chemical analysis ZAF (atomic number-absorption-fluorescence) correction routines were used for matrix corrections.

Back scatter electron imaging was used to document the structures observed at the locations where chemical data were obtained.

### 3.6 CINEMATOGRAPHY

The apparatus for the continuous monitoring of crack path and crack growth rates utilizing cinematography is shown in Figure 13. The loaded WOL sample was placed in the corrosion cell and either single frame or short bursts of 6 to 10 frames were taken on a continuous basis without interruption of the tests. Crack growth rates and crack paths were documented on 16mm Ektachrome film.

The apparatus was also used to monitor crack growth rates by interrupting tests and periodically photographing the crack at predetermined intervals. Crack lengths were measured directly on the film at 20x magnification.

### 3.7 ULTRASONICS

Monitoring of crack extension in fracture toughness tests by ultrasonics was demonstrated by Klima, Fisher and Buzzard (5). The method has also been used successfully for monitoring fatigue crack growth. It has not been used for stress corrosion cracking monitoring. In the present program the signal



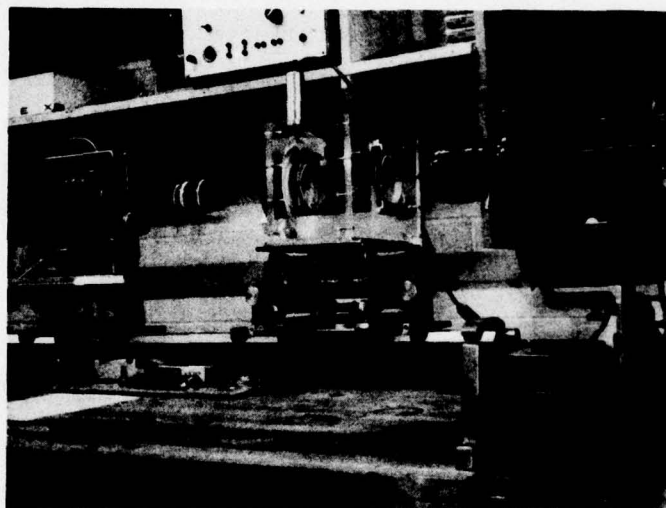


Figure 13. Cinematographic Apparatus Showing Dual 16mm Cameras - WOL Specimen and Corrosion Cell for the Continuous Monitoring of Crack Propagation

transducer pulse-echo technique utilizing longitudinal waves was investigated to determine whether crack movement at the center of the WOL specimen could be monitored in the SCC test. The transducer specimen arrangement and the Krautkramer system are shown in Figure 14. Glycerine was used as a coupling agent for transmitting ultrasonic energy. The transducer was clamped on the top of the specimen and positioned so that the transducer remained out of the corrodant. As the crack propagated, the reflected energy from the crack tip increased and the output voltage at the observed spike increased. The reflected signal was time gated and continuously monitored with a recorder. The rate of increase in the reflected signal from the crack tip was examined in terms of its ability to assess the crack growth rates at the center of the specimen.

Preliminary tests using ultrasonics as a means to monitor crack velocities at the center of the specimen were not successful, primarily because of the edge effects produced by interaction of the ultrasonic beam with the lateral surfaces of the specimen. Reduction of the specimen thickness from 1" to 1/2" in the present series of specimens decreased the ability of the detector to discriminate the center of the specimen from the edges and negated its use as a monitor of the crack velocity at the center of the specimen.

Crack monitoring was restricted to measurement of crack propagation rates at the edges of the specimen during the test and final characterization of the crack front after the test had been completed by examination of the fracture surface. An average value of the crack size used for calculation of  $K_{ISCC}$  is obtained from measurements of the crack length at three locations on the fracture surface.

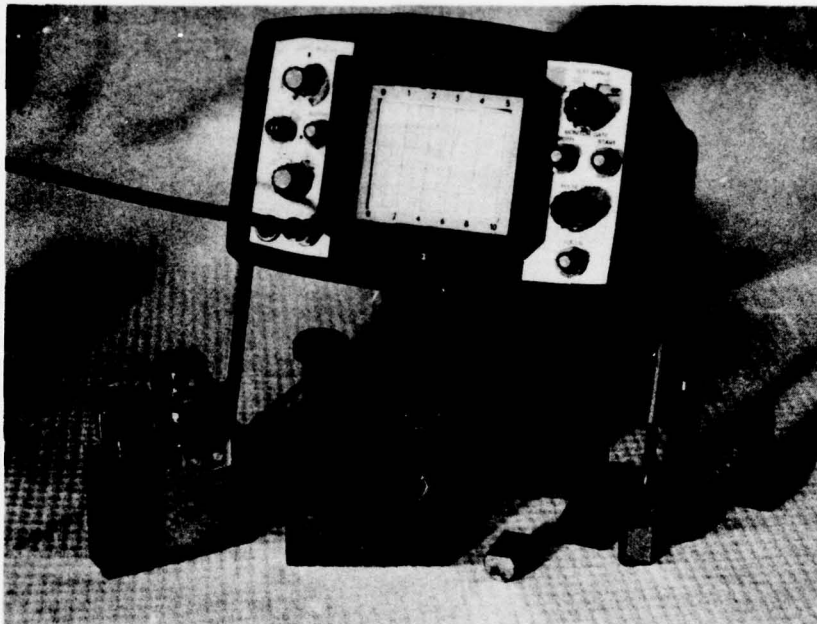


Figure 14. WOL Specimens with Transducer for Ultrasonic Evaluation of Crack Growth and the Krautkramer System



#### 4. RESULTS

##### 4.1 RADIOGRAPHIC TESTS

Welded plates were evaluated for soundness by Magnoflux Corporation according to the ASME Code Sect. 3. The results of their tests are given below.

AF-1410-1	Minor porosity - acceptable
AF-1410-2	Small oxide inclusion at center of weld - avoided in the machining of test samples
AF-1410-3	Minor porosity - acceptable
AF-1410-4	Minor porosity - acceptable
AF-1410-Test	Rejected - Lack of Fusion
AF-1410-5	- acceptable
AF-1410-6	- acceptable
AF-1410-7	- acceptable
AF-1410-8	- acceptable
AF-1410-9	Rejected - Lack of Fusion
AF-1410-10	Not tested

Rejection of test plates was primarily because of lack of fusion in the weld zone.

##### 4.2 MECHANICAL PROPERTIES

The mechanical properties obtained for the fusion zone of the welds of test plates described in Table IV are given in Table V.

Table V. Mechanical Properties of Welds

ITEM	PLATE CONDITION PRIOR TO WELDING	POST WELD TREATMENT	ULTIMATE TENSILE STRENGTH (ksi)	YIELD STRENGTH .2% OFFSET (ksi)	ELONGATION	% RED. IN AREA	CHARPY V-NOTCH FT.-LBS.
1	Aust/WQ	As-Depos.	235.9	206.4	---	65.7	---
2	Aust/WQ	950°F-4 hrs	233.3	223.3	14	62.5	36 to 50
3	950°F-4 hrs	As-Depos.	234.6	209.6		38.5	45 to 61
4	AF-1410-1	As Depos.	224	190.0	14	47.5	56 to 64
5	AF-1410-2	As Depos.	212.5	200	16.5	64.0	78
6	AF-1410-3	As Depos.	230.0	207.5	20.5	65	100
7	AF-1410-4	As Depos.	241.9	205.4	21.0	66.6	55 to 65
8	AF-1410 Test Plate	As Depos.	233.4	213.3	3.2	9.3	66.7
9	AF-1410-5	950°F-4 hrs	219.3	215.3	15	67.3	62
10	AF-1410-6	As Depos.	243.6	220.9	15.6	67.3	61
11	AF-1410-7	950°F-4 hrs		Not	Determined		
12	AF-1410-8	As Depos.		Not	Determined		

Samples AF-1410-1, AF-1410-2 and AF-1410-3 prepared with weld wire from sheet stock exhibited tensile properties slightly lower than those obtained for the base plate in the AFML program. These properties were sufficiently close to the optimum base plate properties, however, to justify stress corrosion cracking evaluation of these samples.

Sample AF-1410-4, AF-1410-5 and AF-1410-6 prepared with the 0.062" dia. weld wire described in Section 3-2 exhibited mechanical properties similar to those reported in AFML-TR-75-148 for "as deposited" welds (Item 3 in Table V.) These results demonstrate the feasibility of utilizing weld wire of the same composition as the base plate to achieve mechanical properties comparable to the base plate.

Low elongation and reduction in area values first obtained for the AF-1410 test plate (Item 8) were attributed to lack of fusion in the weld zone previously detected by Radiographic examination.

Since AF-1410-7 and AF-1410-8 were similar to AF-1410-5 and AF-1410-6, respectively, mechanical properties were not measured for AF-1410-7 and AF-1410-8. Cantilever beam samples prepared from these plates, however, were evaluated for  $K_{ISCC}$  as described in section 4.4.

#### 4.3 (WOL) SCC TESTS IN 3.5% NaCl

Initial (WOL) tests on AF-1410-2 and AF-1410-3 involved 1-T specimens. The first test was conducted on the base plate in the double austenitized and aged condition (950°F - 4 hrs.) and a weld from AF-1410-2 loaded to  $K_{10} = 40 \text{ ksi}\sqrt{\text{in.}}$ . The crack growth was monitored over a period of time extending to 1500 hrs. Sequential photographs comparing the propagation of the cracks on each side of the test sample for the base plate and weld are shown in Figure 15. The crack were first seen to propagate in the base plate after 48 hrs. in test on both sides of the WOL test specimen. No apparent crack movement was observed after the same time in the fusion zone of the weld. Crack branching appeared to occur on both sides of the base plate sample as seen in Figure 15. The double crack continued to propagate through the entire test.




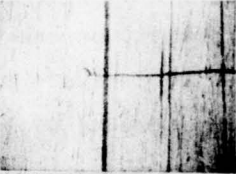

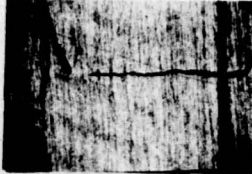
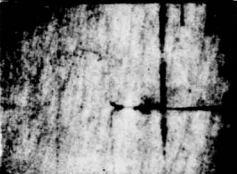
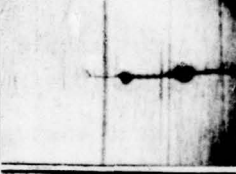








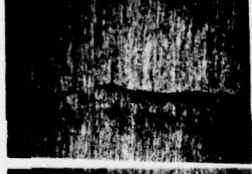

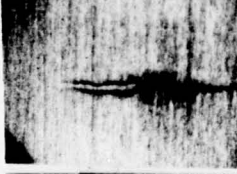















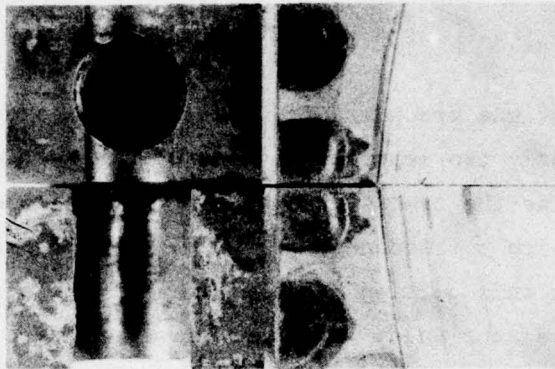
Base Plate		Hrs.	Weld		Date
Side 1	Side 2		Side 1	Side 2	
		0			2/14/78
		24			2/15/78
		48			2/16/78
		480			3/6/78
		504			3/7/78
		528			3/8/78
		648			3/13/78
		696			3/15/78

Figure 15. Crack Propagation in AF-1410-2 Weld and Base Plate  
 $K_{10} = 40 \text{ ksi}\sqrt{\text{in.}}$

Little or no propagation of the crack was observed in the weld zone after 1200 hrs. in test. The development of the irregular crack tip on one side after 48 hrs. was apparently surface related. It showed no evidence of movement throughout the test. Similar observations were repeated by Met Cut Associates who conducted tests on the duplicate sample from AF-1410-2.

After the test, the samples were fractured by cooling the sample with liquid nitrogen. The fatigue and SCC crack fronts observed on the fractured surface are seen in Figures 16(a), (b) and (c) for the weld and base plate.

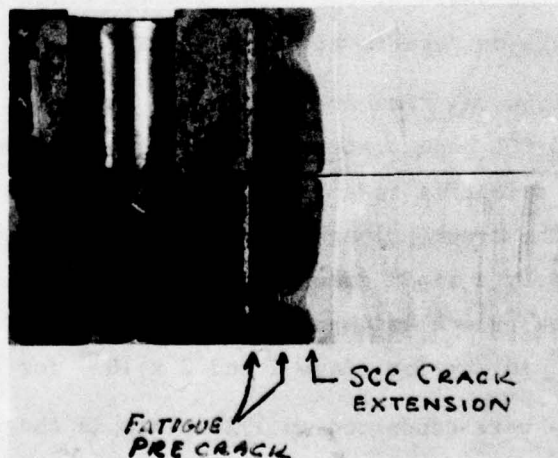
C4708-01



a



b



c

Figure 16. (a) Fracture Surface of AF 1410-2 Weld Tested by MetCut  
(b) Fracture Surface of AF 1410-2 Weld Tested by FIRL  
(c) Fracture Surface of AF 1410 Base Plate Tested by FIRL



Two non-connected fatigue crack fronts were found to be present, as seen in Figure 17(a). Apparently two separate fatigue cracks were nucleated at the notch which did not join as the cracks extended in the weld zone. The central region of the specimen which corresponded to the first weld passes did not propagate suggesting that this portion had a higher fatigue strength than the upper and lower portions of the weld. These observations were also made for AF-1410-3, and suggest that a nonhomogeneous micro-structure or the presence of residual stresses were the cause of the non uniform propagation of cracks in the weld. The crack shapes observed on the fracture surface were similar in both the Met Cut and the FRC tested samples and precluded any meaningful estimates of  $K_{ISCC}$  values for the AF-1410-2 or AF-1410-3 WOL Tests.

The fatigue crack front on the base plate WOL specimen seen in Figure 17(b), however, was uniform and  $K_{ISCC}$  and crack propagation rates could be determined from periodic measurements of the crack lengths measured on the test film. The branching effect observed on the lateral surface of this specimen was apparently associated with the development of a double shear lip at the surface. No evidence of crack branching was observed on the fracture surface.

$K_{ISCC}$  calculated on the basis of the final average crack length measurement on the fracture surface is given in Table VI.

Crack growth extensions vs. time are plotted in Figure 18 for sides 1 and 2 of the 1" thick AF-1410 WOL base plate specimen. A lagging of the crack on side 1 was observed, due primarily to a longer incubation time which preceded the crack propagation. The crack propagation process consisted of an initial incubation stage followed by a rapid growth stage, and then a slow crack growth stage. The rates of crack growth estimated from the slopes of the curves was on the order of  $20 \times 10^{-4}$  in./hr for stage 1 and  $2 \times 10^{-4}$  for stage 2.

Subsequent WOL tests were conducted on 1/2" plate in the aged condition (950°F - 4 hrs.) and in the "as welded" condition as described in Table VI.



Figure 17. (a) Enlarged View of Figure 14(b) Showing Irregular Fatigue Crack Front  
 (b) Enlarged View of Figure 14(c) Showing Fatigue Crack and Sec Crack

Table VI

Specimen	Description	K <sub>10</sub>	K <sub>ISCC</sub>
AF-1410-2	Base Plate (1" TH)	40	32
	Weld (1" TH)	40	Not Evaluated
AF-1410-3	Weld (1" TH)	40	Not Evaluated
AF-1410-4	Test Plate (1" TH)	Not Evaluated	
AF-1410-5	Base Plate (1/2" TH)	15	No Propagation
	Base Plate (1/2" TH)	30	28
	Base Plate (1/2" TH)	45	
	Base Plate (1/2" TH)	60	
	Weld (1/2" TH)	20	No Propagation
	(1/2" TH)	30	22
AF-1410-6	Weld (1/2" TH)	30	Propagation-One Side
	(1/2" TH)	40	Not Evaluated
	(1/2" TH)	45	Not Evaluated



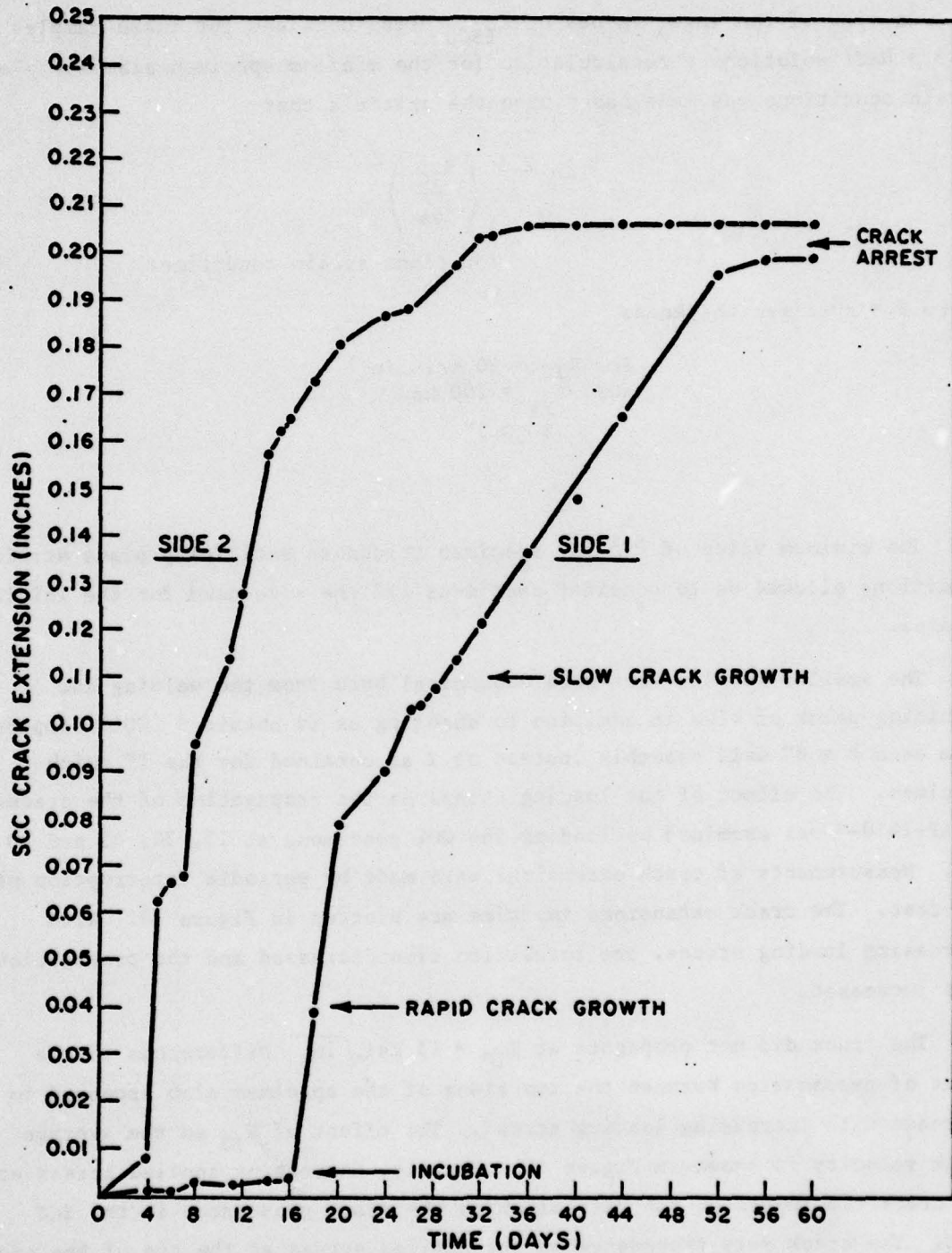


Figure 18. Crack Extension vs. Time WOL Test of AF-1410  
Base Plate  $K_{10} = 40 \text{ ksi}\sqrt{\text{in.}}$

In view of the lower values of  $K_{ISCC}$  being obtained for these samples in 3.5 NaCl solutions a recalculation for the minimum specimen size for plane strain conditions was made based upon the criteria that

$$B \geq 2.5 \left( \frac{K_{IC}}{\sigma_{ys}} \right)^2$$

for plane strain conditions

where  $B$  = specimen thickness

$$\begin{aligned} \text{For } K_{IC} &= 90 \text{ ksi in} \\ \text{and } \sigma_{ys} &= 200 \text{ ksi} \\ B &\geq 0.5'' \end{aligned}$$

The minimum value of 0.5 for specimen thickness satisfying plane strain conditions allowed us to consider specimens 1/2 the size used for the initial studies.

The smaller samples were more economical both from the welding and machining point of view in addition to enabling us to obtain 3 (WOL) samples from each 8 x 8" weld assembly instead of 2 as obtained for the 1" thick specimen. The effect of the loading stress on the propagation of the cracks in AF-1410-5 was examined by loading the WOL specimens at 15, 30, 45 and 60 ksi. Measurements of crack extensions were made by periodic interruption of the test. The crack extensions vs. time are plotted in Figure 19. With increasing loading stress, the incubation time decreased and the propagation rate increased.

The crack did not propagate at  $K_{I0} = 15 \text{ ksi}\sqrt{\text{in.}}$  Differences in the rates of propagation between the two sides of the specimen also appeared to decrease with increasing loading stress. The effect of  $K_{I0}$  on the average crack velocity is shown in Figure 20. Clearly, increasing applied stress at the crack tip increased the rate at which the crack propagated in the SCC test. The crack rate dependence on the applied stress at the tip of the crack may also explain the observed decrease in crack velocity with time.

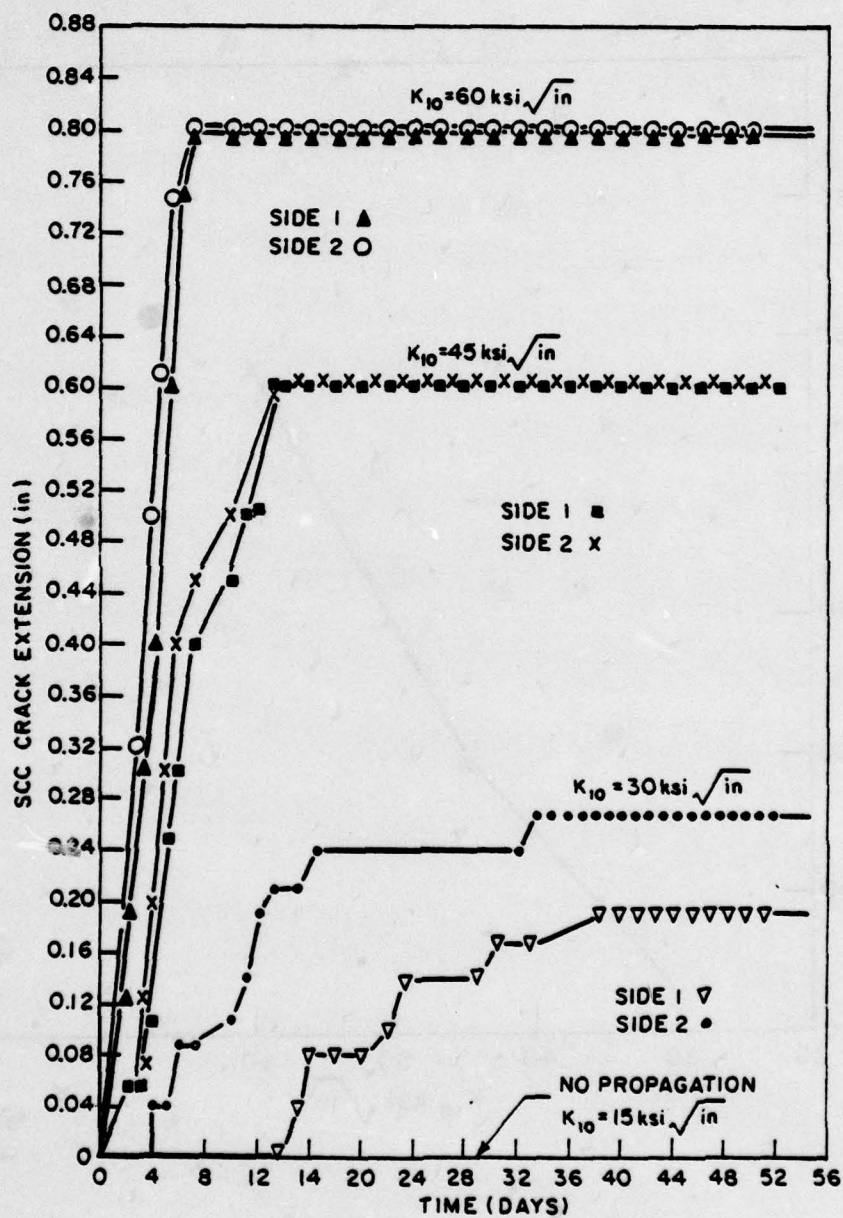


Figure 19. Crack Extension vs. Time WOL Test of AF-1410 Base Plate



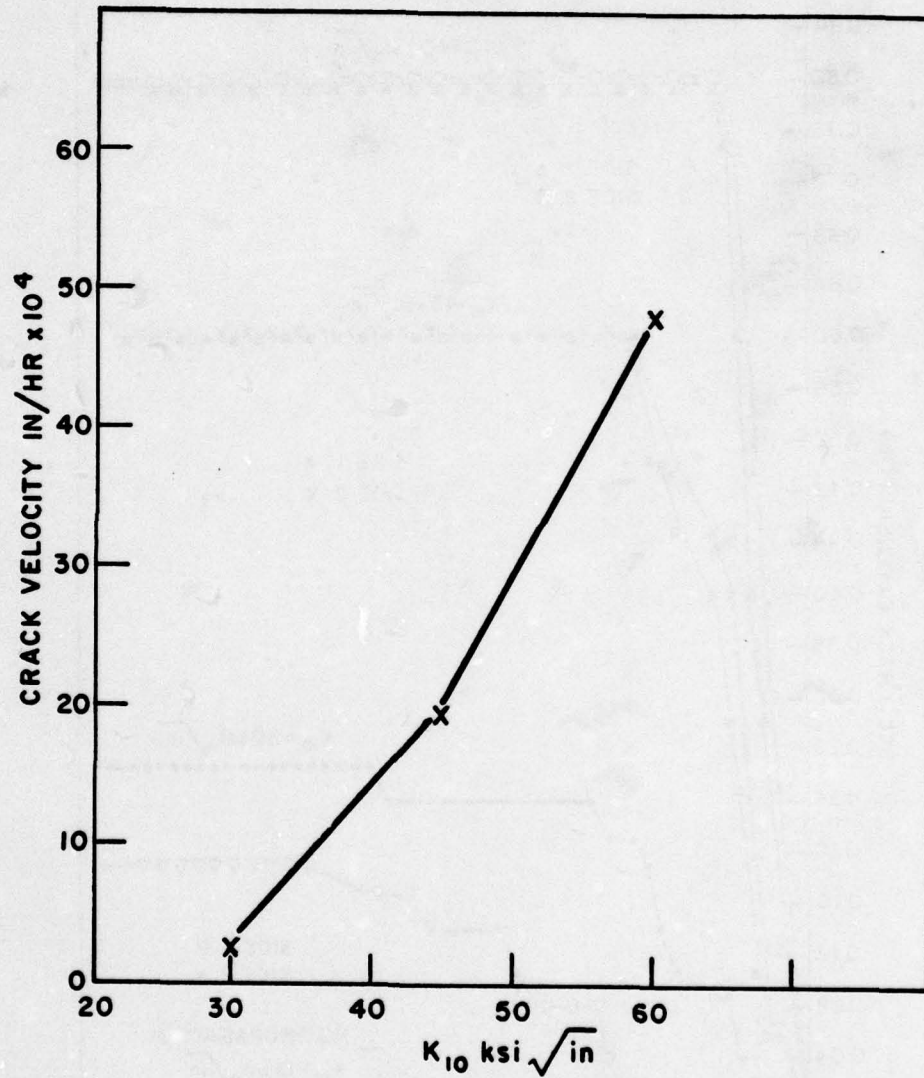


Figure 20. Effect of  $K_{10}$  on Average Crack Velocity AF-1410 Base Metal Aged ( $950^{\circ}\text{F}$  - 4 hrs.) from Figure 19

The estimated  $K_{ISCC}$  value calculated on the basis of the final average crack length observed in the fracture surface is given in Table VI. The value of 28 ksi  $\sqrt{\text{in.}}$  was only slightly lower than the value of 32 ksi  $\sqrt{\text{in.}}$  obtained for the 1" thick WOL test in AF-1410-2 and it is not known whether the difference is related to thickness difference or to normal scatter in the data since only one test was conducted on the 1" thick plate.

Crack extension vs. time for AF-1410-5 welds are shown in Figure 21. These specimens were loaded at  $K_{10} = 20$  and 30 ksi  $\sqrt{\text{in.}}$  as shown in Table VII. The crack did not propagate after approximately 1500 hrs. at  $K_{10} = 20$  ksi  $\sqrt{\text{in.}}$ . At  $K_{10} = 30$  ksi crack movement was observed after an incubation time of from 280 to 380 hrs. The crack then propagated rapidly initially and slowed down before arresting after about 670 to 790 hrs.  $K_{ISCC}$  calculated on the basis of the average crack length observed on the fracture surface was equal to 22 ksi  $\sqrt{\text{in.}}$ .

WOL Tests in AF-1410-6 welds resulted in non uniform crack propagation through the weld as seen on the fracture surfaces in Figure 22 and similar to those observed for AF-1410-2 and AF-1410-3 in Figure 16 and 17. In contrast to these findings, the crack front observed for AF-1410-5 weld and base plate were much more uniform as seen in Figure 23. Aging of the latter plate after welding may have reduced the residual stresses and produced a more uniformly aged structure than the "as welded" structure present in AF-1410-2, AF-1410-3 and AF-1410-6.

#### 4.4 CANTILEVER BEAM (CB) SCC TESTS

The results of (CB) SCC Tests are given in Table VII. The first sample from AF-1410-7 weld was loaded to  $K_{10} = 40$  ksi  $\sqrt{\text{in.}}$ . It failed after 48 hrs. A second specimen loaded at  $K_{10} = 34$  ksi  $\sqrt{\text{in.}}$ , failed after 168 hrs. The third specimen loaded at  $K_{10} = 15$  ksi  $\sqrt{\text{in.}}$  showed no signs of movement after approximately 1100 hrs. The load was then incrementally increased from  $K_{10} = 15$  ksi  $\sqrt{\text{in.}}$  to  $K_{10} = 32$  ksi  $\sqrt{\text{in.}}$  where failure occurred after 1700 hrs. The estimated  $K_{ISCC}$  for AF-1410-7 was between  $K_{ISCC} = 30$  to 32 ksi  $\sqrt{\text{in.}}$ . This value may be compared with (WOL)  $K_{ISCC} = 22$  ksi  $\sqrt{\text{in.}}$ , obtained for the AF-1410-5 weld, which was similarly heat treated.

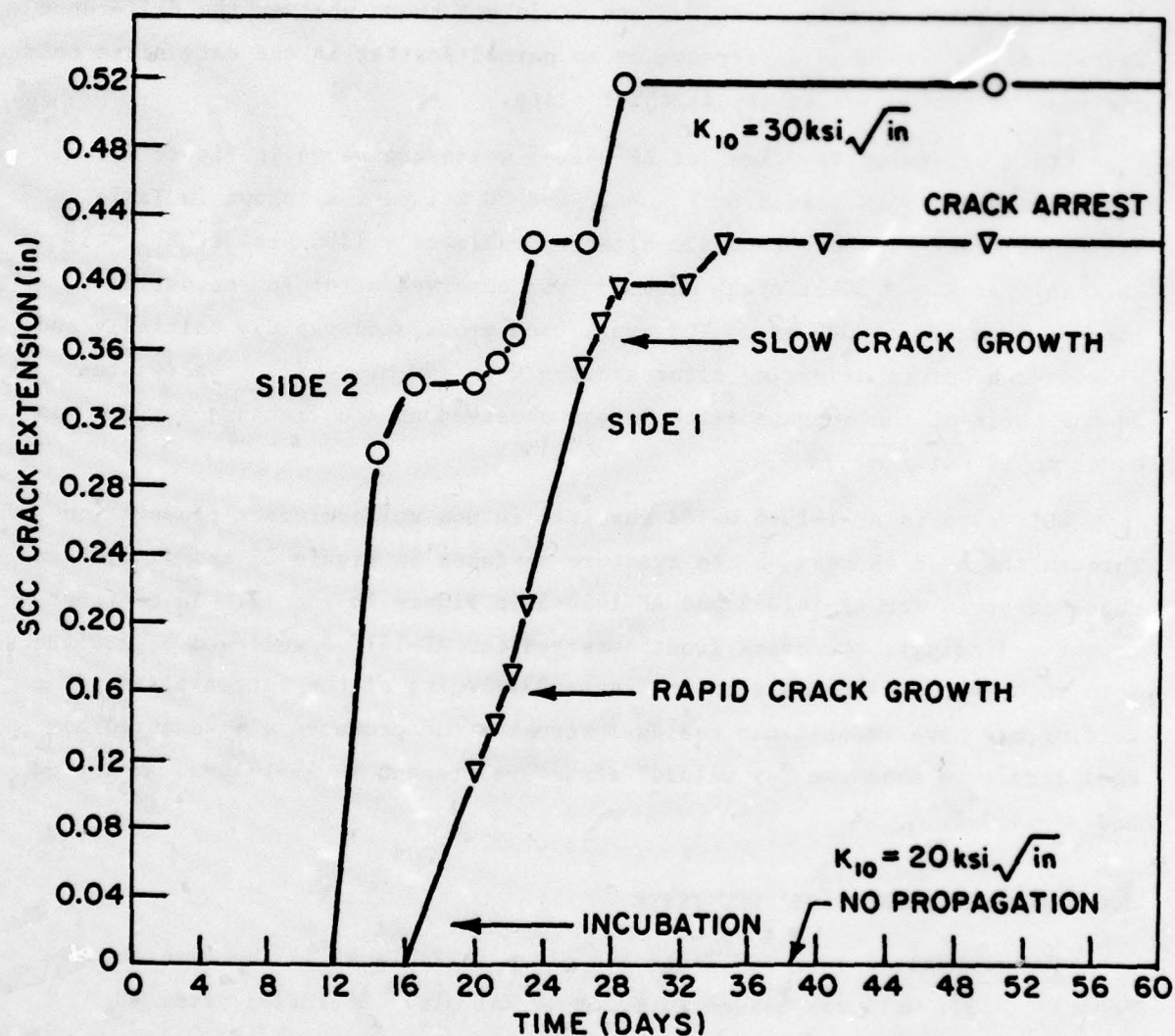
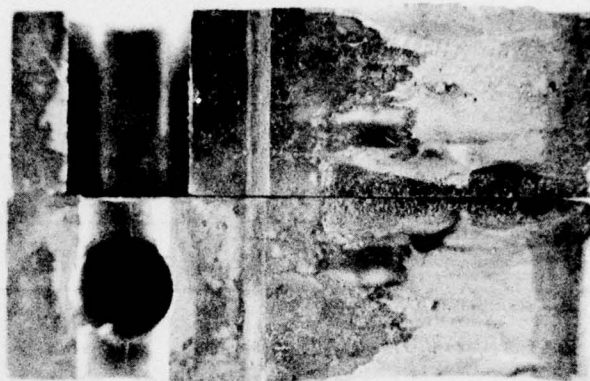


Figure 21. Crack Extension vs. Time WOL Test  
AF-1410-5 (Weld)  $K_{10} = 30 \text{ ksi}\sqrt{\text{in.}}$

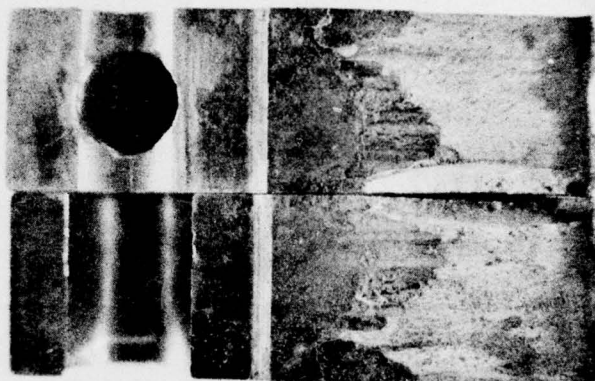


Table VII. Cantilever Beam Tests

SAMPLE		$K_{I0}(\text{ksi}\sqrt{\text{in}})$	TIME (HRS)	FAILURE
AF-1410-7 in 3.5% NaCl in H <sub>2</sub> O	W1	40	48	Yes
	W2	34	161	Yes
	W3	15	1,100	No
	W3	25	1,400	No
	W3	30	1,536	No
	W3	32.5	1,700	Yes
AF-1410-8 in 3.5% NaCl in H <sub>2</sub> O	W1	50	48	Yes
	W2	30	300	No
	W2	40	1,432	No
	W2	47.5	1,744	Yes
AF-1410-8 in Moist Air	W1	70	720	No
		80	984	No
		90	1,200	No



(b)



(c)



(a)

Figure 22. Fractured Surface of WOL Specimen AF-1410-6 at Weld. Irregular Fatigue and SCC Crack Fronts.

(a)  $K_{10} = 30 \text{ ksi}\sqrt{\text{in}}$

(b)  $K_{10} = 40 \text{ ksi}\sqrt{\text{in}}$

(c)  $K_{10} = 45 \text{ ksi}\sqrt{\text{in}}$



(a)



(b)

Figure 23. Fracture Surface of AF-1410-5 WOL (a) Base Plates and (b) Weld Specimens Showing Fatigue and SCC Crack Fronts



The results of (CB) SCC tests for AF-1410-8 are also given in Table VII. Failure occurred at a  $K_{I0} = 50 \text{ ksi}\sqrt{\text{in.}}$  after 48 hrs. No failure occurred at  $K_{I0} = 40 \text{ ksi}\sqrt{\text{in.}}$  after 1432 hrs. Failure occurred for  $K_{I0} = 47.5 \text{ ksi}\sqrt{\text{in.}}$  after 1744 hours. The  $K_{ISCC}$  value was estimated to be between 45 and 47.5  $\text{ksi}\sqrt{\text{in.}}$ . In comparison to these results, the (WOL) test previously described for AF-1410-6 showed no crack extension on one side of the specimen even at  $K_{I0} = 45 \text{ ksi}\sqrt{\text{in.}}$ , but propagation on the other side occurred at  $K_{I0} = 30 \text{ ksi}\sqrt{\text{in.}}$ . The higher value of  $K_{ISCC}$  obtained for AF-1410-8 than for AF-1410-7 suggests that the "as welded" specimen was more stress corrosion crack resistant due mainly to inhomogeneities in the microstructure or to the presence of residual stresses introduced by welding.

The cantilever beam test appears to be better suited for the evaluation of a  $K_{ISCC}$  value for the nonhomogeneous welds since it established a maximum stress level required to propagate the crack to failure, whereas (WOL) tests reflected the stresses at which the cracks were arrested. Nonuniformities in the structure produced nonuniform crack fronts not amenable to calculation of  $K_{ISCC}$ .

One final test on AF-1410-8 weld was conducted in a moist air environment. Air at room temperature saturated with moisture was passed over the specimen throughout the test period. At  $K_{I0} = 90 \text{ ksi}\sqrt{\text{in.}}$ , no failure was observed after 1200 hrs. This was the maximum value of stress for the 1/2" thick specimen satisfying plane strain conditions. Time did not permit the evaluation of  $K_{ISCC}$  in the moist air environment with additional tests.

#### 4.5 METALLURGICAL AND CHEMICAL HOMOGENEITY OF WELDS

The fusion zone of weld cross sections as seen in Figures 24(a), (b) and (c) were studied with the SEM for both metallurgical and chemical homogeneity. The compositional and hardness variation observed in the cross sections from top to bottom of the fusion zones are given in Tables VIII to XII for AF-1410-2, AF-1410-3, AF-1410-4, AF-1410-5, and AF-1410-6 respectively. The region designated top of weld represents the final passes of the weld.

C4708-01

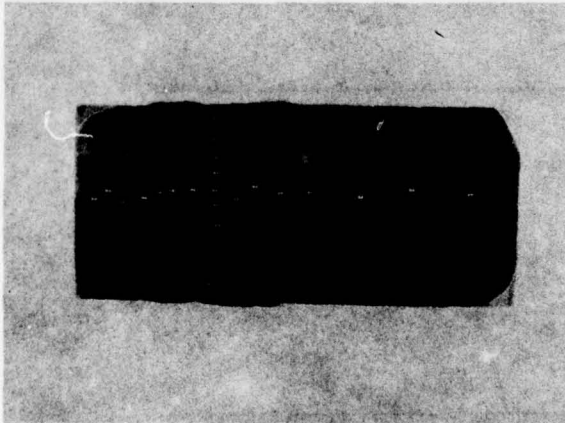
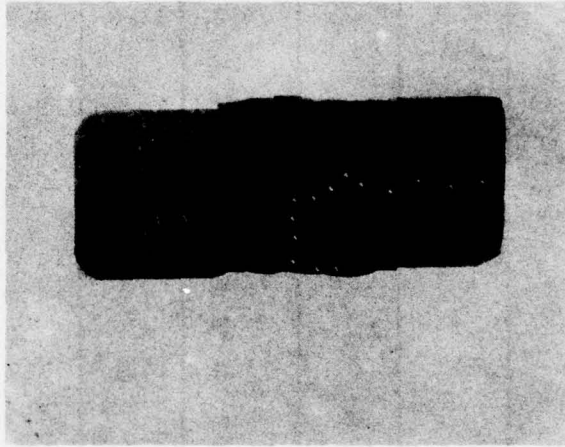
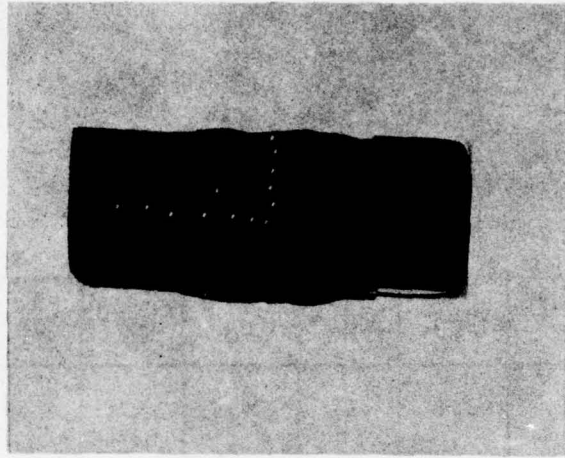


Figure 24. Weld Cross Sections with Hardness Impressions  
(a) AF 1410-2  
(b) AF 1410-3  
(c) AF 1410-4

Table VIII. AF-1410-2

<u>Location</u>	Hardness $R_c$	Cr	Mn	Fe	Co	Ni	Mo
Weld 1	42.6	1.8	.01	74.5	13.4	9.8	1.5
Weld 2	44.0	1.8	.01	74.2	13.9	9.8	1.2
Weld 3	46.4	1.9	.02	74.2	14.0	9.9	1.0
Weld 4	46.4	2.0	.01	73.4	14.8	9.4	1.0
Weld 5	44	1.7	.03	73.2	14.1	9.7	1.3
Weld 6	45	1.9	.01	72.8	13.3	9.8	1.0
Base Plate 7	45.2	1.9	.01	74.0	14.1	9.9	1.0
Base Plate 8	45	2.1	.01	74.0	14.3	9.2	1.4

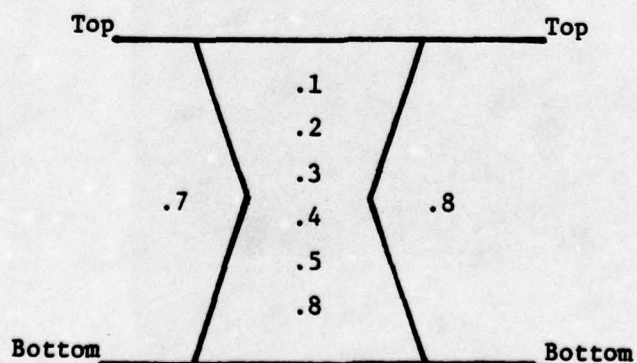




Table IX. AF-1410-3

Location	Hardness $R_c$	Cr	Mn	Fe	Co	Ni	Mo
Weld 1	41.5	1.9	0.01	72.8	13.6	9.2	0.7
Weld 2	44.5	1.8	0.01	71.3	13.9	9.2	1.0
Weld 3	42.5	2.0	0.01	74.3	13.7	9.2	1.1
Weld 4	44.5	1.9	0.03	72.9	14.2	9.3	1.0
Weld 5	44.1	1.9	0.03	72.5	14.2	8.7	1.1
Weld 6	44.9	2.0	0.01	74.2	14.4	9.5	.7
Base Plate 8	45.2	2.0	0.01	72.8	14.0	9.3	1.1
Base Plate 9	45.0	1.9	0.03	73.6	14.7	9.2	1.2

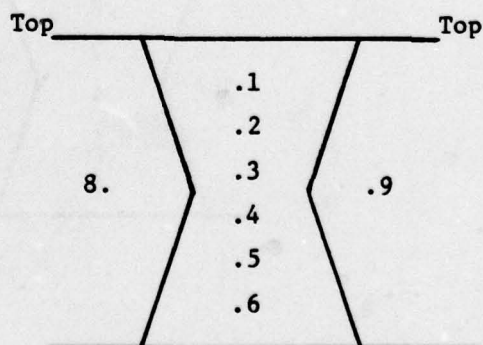


Table X. AF 1410-4

Location	Hardness R <sub>C</sub>	Cr	Mn	Fe	Co	Ni	Mo
Weld 1	48	1.9	0.07	72.7	13.2	8.8	1.0
Weld 2	49.5	1.9	0.01	74.4	14.2	9.1	.8
Weld 3	48.5	2.1	0.01	74.7	13.6	9.2	.2
Weld 4	45.5	2.1	0.01	77.9	14.6	9.8	.5
Weld 5	51.0	2.0	0.01	77.4	14.2	9.0	1.5
Weld 6	49.5	1.9	0.01	77.0	14.0	9.8	1.0
Base Plate 7	47	1.9	0.01	75.0	14.2	9.8	1.4
Base Plate 8	47.5	2.1	0.01	77.1	14.1	9.6	1.2

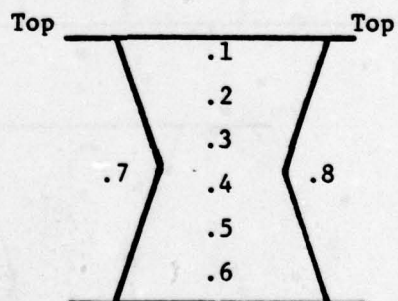


Table XI. Hardness Measurements and Compositional Variation on Cross Section of Weld from AF-1410-5

Location	Hardness $R_C$	Composition					
		Cr	Mn	Fe	Co	Ni	Mo
1 - Weld	43	1.7	<0.01	70.0	13.7	9.6	1.0
2 - Weld	45	1.8	<0.01	71.2	14.0	9.3	1.2
3 - Weld	45	1.7	<0.01	71.8	13.9	9.6	1.2
4 - Weld	45	1.9	<0.01	71.3	14.2	9.4	1.0
5 - Weld	43	1.9	<0.01	72.2	14.1	9.5	1.0
6 - Weld	43	1.8	<0.01	71.9	14.3	9.6	1.0
7 - Weld	44	2.0	<0.01	72.5	14.0	9.8	1.1
8 - HAZ	46	2.0	<0.01	73.4	14.1	9.8	1.1
9 - Base Plate	44	1.9	<0.01	71.4	14.0	9.4	1.0

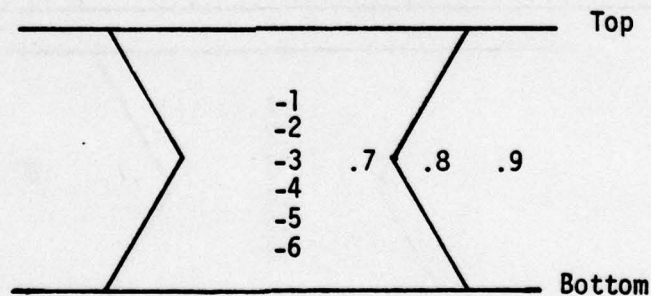
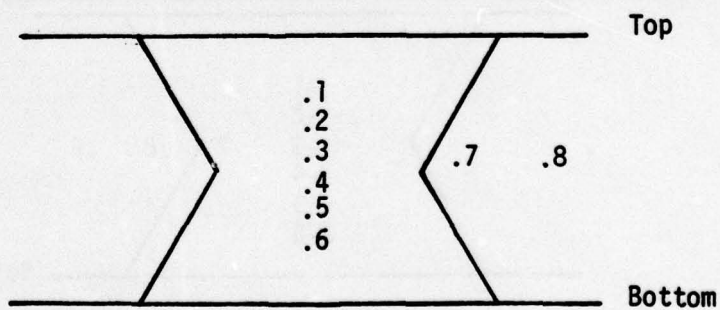




Table XII. Hardness Measurements and Compositional Variation on Cross Section of Weld from AF-1410-6

Location	Hardness $R_C$	Composition					
		Cr	Mn	Fe	Co	Ni	Mo
1	41	1.8	0.01	73.2	13.9	10.0	1.1
2	43	1.9	0.01	73.5	13.9	9.7	0.9
3	50	1.7	0.01	72.5	13.7	9.3	1.0
4	46	2.0	0.01	73.0	14.0	9.7	1.0
5	45	1.9	0.01	73.0	13.9	10.0	1.0
6	48	2.0	0.01	73.0	14.0	9.7	0.7
7 - HAZ	48	1.8	0.01	73.0	14.1	10.0	1.0
8 - Base Plate	50	1.9	0.01	72.9	13.9	10.1	1.0

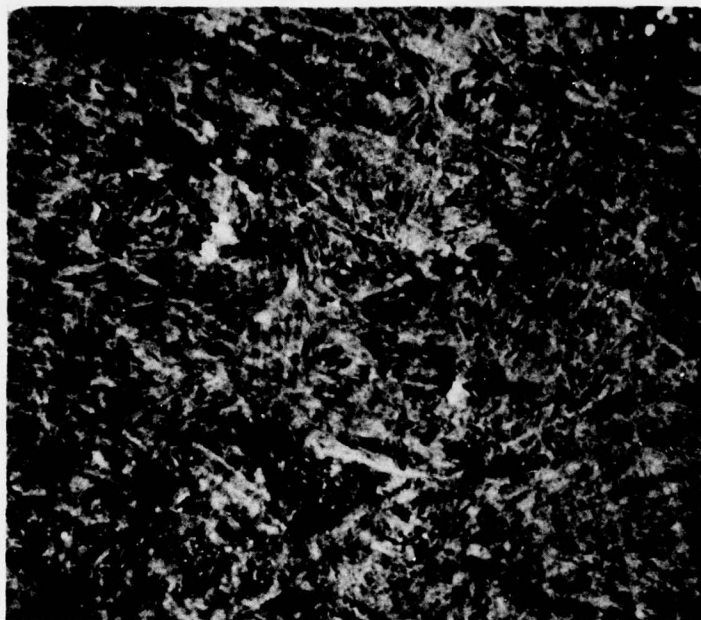


The compositional variation of Cr, Mn, Fe, Co, Ni and Mo through the weld zone for each of the weld assemblies was found to be minimal. The Mo content for AF-1410-4 was lower than observed for the other welds at position 3 and 4 in the weld.

The hardness tended to be lower at the top position for all of the weld assemblies except for AF-1410-5, which appeared to show more uniformity in hardness than any of the other welds. The variation of hardness in the weld cross section may reflect nonuniformity in aging associated with the "as welded" condition.

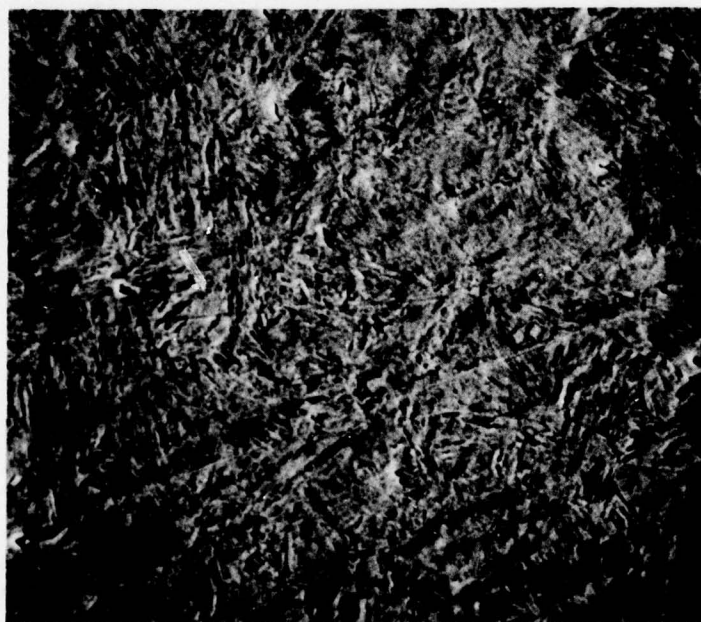
Back scattered SEM micrographs of the microstructures observed at the various locations at which hardnesses were taken from AF-1410-2 and AF-1410-5 shown in Table VIII are shown in Figures 25 to 30.

The microstructure of AF-1410-2 weld consisted of a coarser lath martensite with microporosity than observed for AF-1410-5 as noted in comparing Figures 25, 26 and 27 to Figures 28, 29 and 30. The refinement of the martensite and grain size was achieved by preheating the plates prior to welding. In addition to structure refinement the structure also appeared to be more uniform throughout the weld cross section. To minimize residual stresses, the direction of welding was reversed after each pass. It was not possible to assess the effectiveness of the latter procedure in minimizing residual stresses since the measurement of residual stresses in the cross section was beyond the scope of the program.



C4708-01

1



2

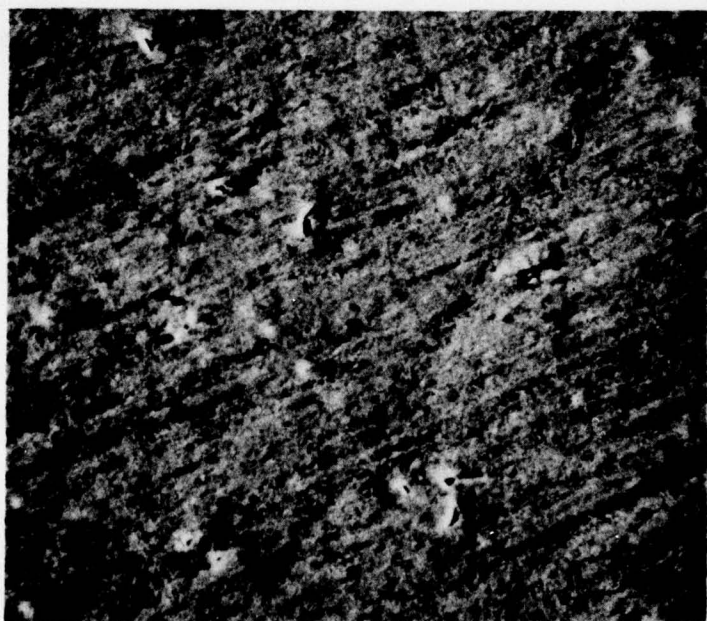
Figure 25. Back Scattered Electron Image of Weld AF-1410-2 at Positions 1 and 2 Shown in Table V. Mag. 500X





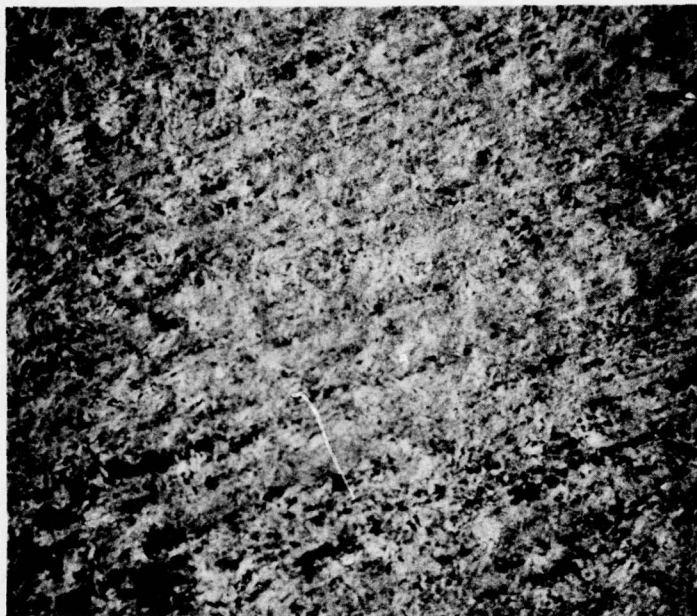
C4708-01

3

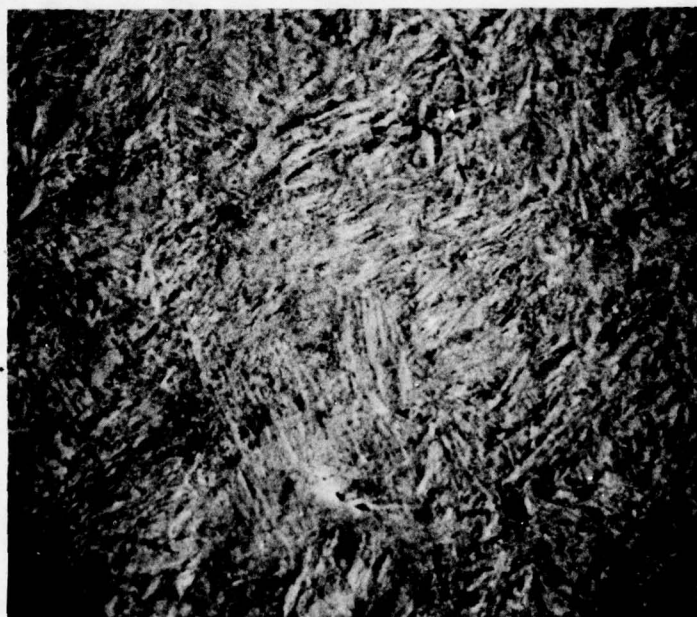


4

Figure 26. Back Scattered Electron Image of Weld AF-1410-2 at Positions 3 and 4 Shown in Table V. Mag. 500X



C4708-01  
5



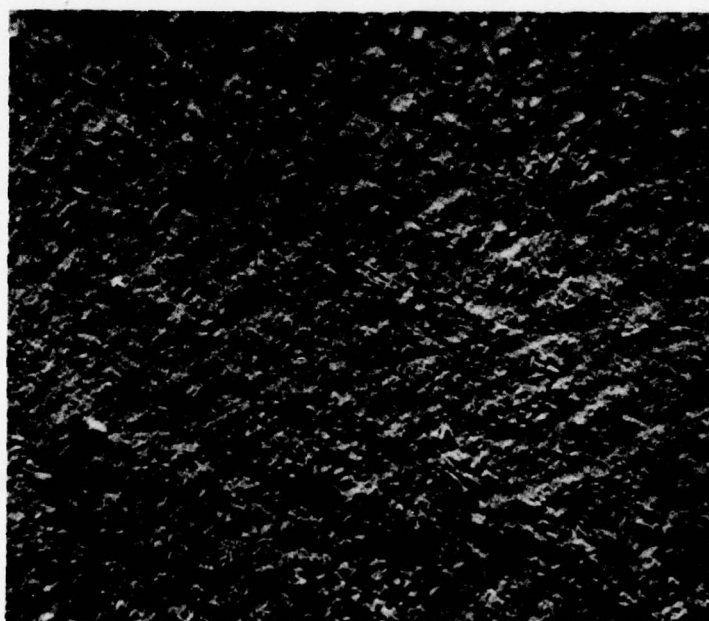
8

Figure 27. Back Scattered Electron Image of Weld AF-1410-2 at Positions 5 and 8 Shown in Table V. Mag. 500X



C4708-01

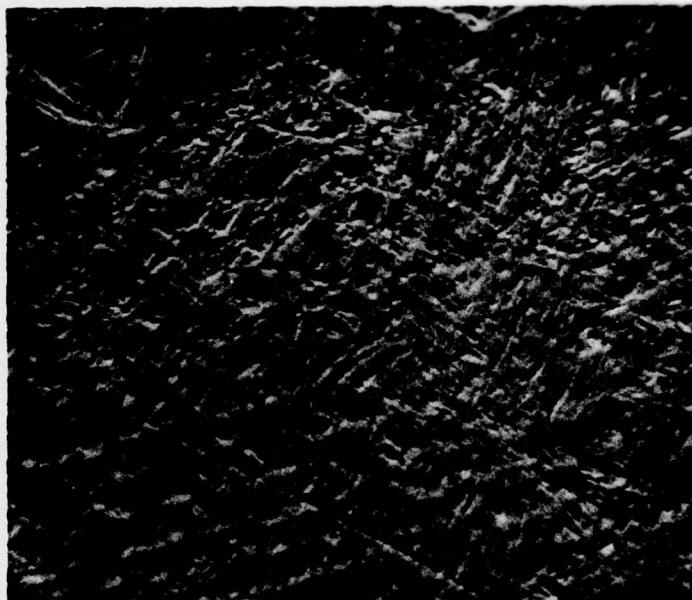
1



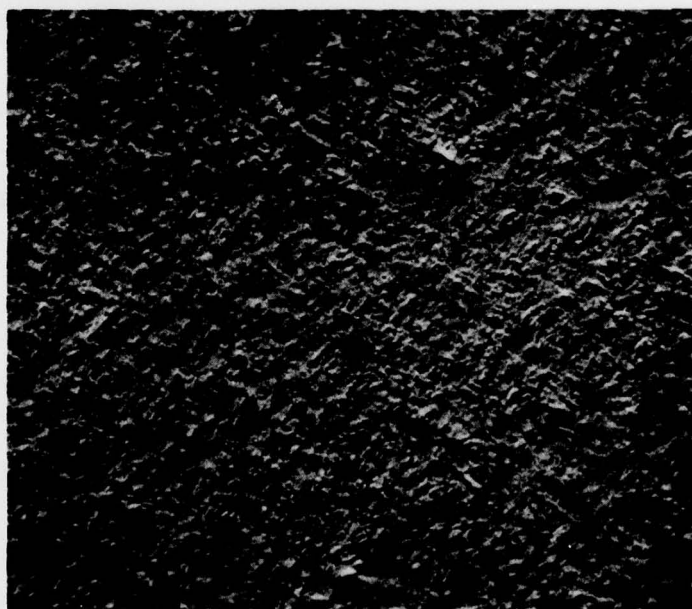
2

Figure 28. Back Scattered Electron Images of Weld AF-1410-5 at Positions 1 and 2 Shown in Table VI. Mag. 500X



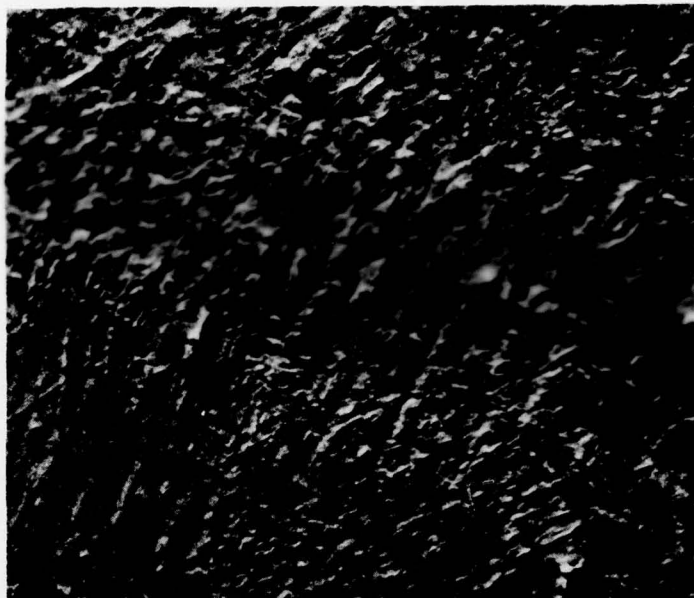


C4708-01 3

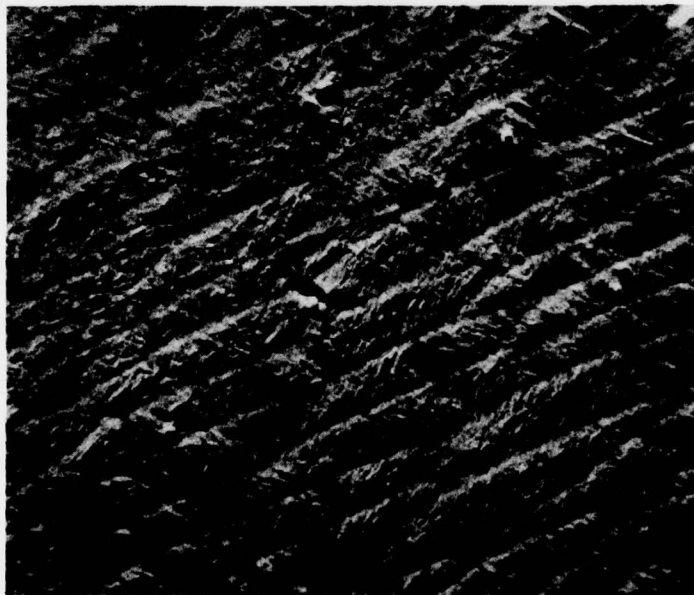


4

Figure 29. Back Scattered Electron Images of Weld AF-1410-5 at Positions 3 and 4 Shown in Table VI. Mag. 500X



C4708-01 5



6

Figure 30. Back Scattered Electron Images of Weld AF-1410-5 at Positions 5 and 6 Shown in Table VI. Mag. 500X

## 5. DISCUSSION & SUMMARY

The present findings show that manual CW-GTA welds obtained by using filler metal prepared from AF-1410 sheet stock or from 0.062 dia. wire prepared from AF-1410 base plate and having the same nominal composition as the base plate can produce welds having mechanical and stress corrosion cracking properties similar to those of the base plate. The yield strength variation from 190 to 221 ksi and ultimate tensile strength from 212 to 244 ksi observed for some welds met the minimum mechanical property requirements of 220 (TY) and 230 (UTS) specified as the goal in the AFML-TR-75-148 program.

Stress corrosion cracking data obtained for the base plate in the aged ( $950^{\circ}\text{F}$  - 4 hrs.) condition using WOL specimens yielded values of  $K_{\text{ISCC}} = 28 \text{ ksi} \sqrt{\text{in.}}$  for 1/2" plates and  $K_{\text{ISCC}} = 32 \text{ ksi} \sqrt{\text{in.}}$  for 1" thick plates. These results were much lower than initially reported values of  $100 \text{ ksi} \sqrt{\text{in.}}$  and in closer agreement with data reported of Rockwell International of  $30 \text{ ksi} \sqrt{\text{in.}}$

$K_{\text{ISCC}}$  values for welds prepared in the present work varied from  $32 \text{ ksi} \sqrt{\text{in.}}$  to  $47.5 \text{ ksi} \sqrt{\text{in.}}$  for the welded and aged ( $950^{\circ}\text{F}$  - 4 hrs) to the "as welded" condition, respectively, measured by the cantilever beam method. The (WOL) method yielded  $K_{\text{ISCC}} = 22 \text{ ksi} \sqrt{\text{in.}}$  for the weld in the aged condition.

Nonhomogeneities in the "as welded" structure can contribute to erroneous SCC data for (WOL) specimens since the method of test may cause the arresting of cracks at discontinuities in the microstructure and result in an irregular crack front.

At low stresses only slightly higher than the  $K_{\text{ISCC}}$  level differences in the rate of crack propagation were observed on the two sides of the specimen. At higher stresses, however, these differences tended to diminish since discontinuities were not able to arrest the crack under the influence of the increased stress at the crack tip.



The average SCC velocity in AF-1410 base plate increased from  $2 \times 10^{-4}$  in./hr. to approximately  $50 \times 10^{-4}$  in./hr. with increasing stress. The stress dependence of crack velocity may account for the diminishing of crack velocity with time in the WOL test.

The cantilever beam test appears to offer a more effective method to evaluate materials which may tend to be nonhomogeneous, such as welds, since it measures the maximum stress level required to propagate a crack to failure. Minor discontinuities become ineffective barriers to the propagating crack under the influence of an increasing stress.

A single test conducted in moist air suggested that appreciably higher values of  $K_{ISCC}$  should be encountered in inert gaseous environments. The effects of corrosive gaseous environments such as those containing  $SO_2$ ,  $H_2$  or  $H_2S$  have not been examined but may be significant in future evaluations of AF-1410 for aircraft applications.

## 6. STATUS AND SIGNIFICANCE OF RESEARCH EFFORT

The significant accomplishments made toward achieving the research objectives describes in Section 2 are summarized below.

1. Commercially available AF-1410 plates were welded using GTA cold wire manual feed with commercially available 0.062 AF-1410 wire originating from the same starting material as the base plates. Prior work had suggested that additions of 0.1 to 0.2% Si and up to 0.02%Al and 0.10%V were necessary in the weld wire to prevent porosity in the welds and to achieve optimum mechanical properties. By controlling the welding parameters and assuring adequate shielding of the weld, high quality welds were prepared which exhibited mechanical properties equivalent to the base plate using filler rods of the same composition as the base plates.

2. The welds were carefully evaluated and screened using radiographic, scanning electron microscopy and mechanical tests prior to conducting stress corrosion cracking tests.

3. Both WOL and CB specimens were tested to determine the stress corrosion cracking sensitivity of the welds and base plate in 3.5% NaCl solutions.

$K_{ISCC}$  values of from 20 to 30  $\text{ksi}\sqrt{\text{in}}$  obtained in this program for both welds and base plate were appreciably lower than values of 60 to 100  $\text{ksi}\sqrt{\text{in}}$  initially reported for laboratory melted AF-1410 and were more in agreement with values of 30  $\text{ksi}\sqrt{\text{in}}$  reported by Rockwell International. Seemingly high values of  $K_{ISCC}$  associated with welds appeared to be associated with non-uniformity in the metallurgical structure of the weld which resulted in a non-uniform crack front.

4. A cinematographic system of studying crack propagation was used to evaluate crack growth rates under various conditions of loading of WOL specimens. Crack velocities were found to depend upon the loading stress at

$K_{10}$  values close to the  $K_{ISCC}$  value, the average crack growth rate was  $2 \times 10^{-4}$  inches/hr. It increased to  $50 \times 10^{-4}$  inches/hr at a loading stress of 60 ksi $\sqrt{\text{in}}$ .

5. Limited testing of welds to evaluate stress corrosion cracking sensitivity in moist air was conducted. These preliminary tests suggested that appreciably higher values of  $K_{ISCC}$  should be encountered in inert gaseous environments than observed in 3.5% NaCl solution.

The author feels however that further testing in corrosive gaseous environment such as those containing  $\text{SO}_2$ ,  $\text{H}_2$  or  $\text{H}_2\text{S}$  should be conducted to fully evaluate the susceptibility of this alloy to stress corrosion cracking in aircraft applications.

6. Through this research grant, FRC is now in a position to conduct further research in this important area of stress corrosion cracking of metals and welds combining WOL, CB and Cinematographic analysis of crack propagation.

7. Although these data have not been published to date, the author feels that his continued interest in this field of stress corrosion cracking will lead to several publications on this subject. The present findings will be incorporated in these future publications.

8. Dr. Damiano consulted with Dr. J. T. Cammett in the evaluation of standard practices used for stress corrosion cracking susceptibility measurements and visited MetCut Research while SCC tests were being conducted for Universal Cyclop on AF-1410. He was also in frequent communication with R. R. Shiring, J. L. Milavec and H. L. Black Universal Cyclops during the preparation and development of the weld wire for this program from June 1977 to June 1978.

9. There were no inventions or patent disclosures stemming from this research effort although the specific application of wire fabricated from AF-1410 production stock for filler material is significant since it demonstrated that a specially prepared ingot was not needed for weld wire to produce acceptable welds in AF-1410.



10. The accomplishments of this research program are significant since they deal with the stress corrosion cracking behavior of welds prepared with commercially available AF-1410 for which appreciable data have been accumulated. These data may be usable for future design consideration or for continued future work on this alloy in its application as a structural aircraft material.

#### ACKNOWLEDGEMENTS

This is to acknowledge the assistance of Mr. Hugh Kelly in the welding of AF-1410 plates, Mr. Louis Cinquina for his assistance in the conducting of the stress corrosion cracking tests and the setting up of the equipment, and Richard Fiore and Thomas Tucker for their contribution in the scanning electron microscopy studies.



## REFERENCES

1. Routh, W. E., "Lower Cost by Substituting Steel for Titanium", AFFDL-TR-77-73, under Contract F33615-75-C-3109.
2. Novak, S. R. and Rolfe, S. T., "Modified WOL Specimen for K<sub>I</sub>SCC Environmental Testing", Journal of Materials JMLSA, Vol. 4, No. 3, Sept. 1969, pp. 701-728.
3. Fisher, D. M., Bubsey, R. T. and Srawley, J. E., "Design and Use of Displacement Gage for Crack Extension Measurements", NASA TN D-3724, NASA Research Center, Cleveland, Ohio.
4. Brown, B. T., "A New Stress Corrosion Cracking Test for High Strength Alloys", Materials Research and Standards, Vol. 6, No. 3, March 1966, pp. 129-133.
5. Klima, S. J., Fisher, D. M. and Buzzard, "Monitoring Crack Extension in Fracture Toughness Tests by Ultrasonics", Journal of Testing and Evaluation, Vol. 4, No. 6, Nov. 1976, pp. 397-404.



# APPENDIX

C4708-01

A

FRACTURE MECHANICS APPROACH TO SCC



**Franklin Research Center**

A Division of The Franklin Institute

The Benjamin Franklin Parkway, Phila., Pa. 19103 (215) 448-1000

## FRACTURE MECHANICS APPROACH TO SCC

The fracture mechanics approach is generally used as the most reliable method to establish the sensitivity of materials to stress corrosion cracking. The resistance of high strength steels to sea water stress corrosion cracking is characterized in terms of a threshold level of stress intensity below which SCC does not occur. The threshold level of stress intensity, defined in linear elastic fracture mechanics as  $K_{I\text{ SCC}}$ , combines the threshold and flaw size and may be compared directly to the fracture stress intensity parameter  $K_{Ic}$  determined in air under plane strain condition as established by ASTM Committee E-24.

Although no standard method of test has been adopted to determine  $K_{I\text{ SCC}}$ , two techniques have been widely used and accepted as valid methods of test.

One method developed by Brown [1] is the cantilever bend test. This method employs a pre-fatigue notched bar held horizontally and surrounded at the notch by the corrodant in a molded polyethylene container. The specimen is dead weight for periods of time extending to a minimum time of 500 hours under a fixed load.

The stress intensity factor  $K_\alpha$  is calculated for each condition of loading as a function of time to fracture using the following relationship

$$K_\alpha = \frac{4.12M (\alpha^{-3} - \alpha^3)^{1/2}}{BD^{3/2}}$$

where M is the bending moment

B is the breadth of the specimen

$$B \geq 2.5 \left( \frac{K_{Ic}}{\sigma_{ys}} \right)^2 \quad \text{for}$$

plane strain



D is the vertical depth of the specimen

$\alpha$  is defined as  $1 - \frac{a}{D}$  where a is the total initial depth of the notch plus fatigue cracking.

$K_{I\text{ SCC}}$  is defined as the value of  $K_{I\alpha}$  below which the specimen does not fail after an extended time in excess of 500 hours. Six specimens are generally required to evaluate one value of  $K_{I\text{ SCC}}$ .

A second method, developed by Novak and Rolfe [2] utilizes a modified wedge opening loading (WOL) specimen. In contrast to the cantilever bend test, the modified (WOL) test is a constant displacement test which utilizes a single precracked specimen. This latter method eliminates the need for a special fixture and facilitates the simultaneous testing of numerous specimens.

The applied  $K_I$  value at the tip of the crack is calculated using the following equation.

$$K_I = \frac{PC_3 \left( \frac{a}{w} \right)}{B(a)^{1/2}}$$

Where P = load

a = crack length

w = specimen width

B = specimen thickness

$C_3 \left( \frac{a}{w} \right)$   $C_3$  function of  $\left( \frac{a}{w} \right)$ ,

is given by

$$C_3 \left( \frac{a}{w} \right) = \left[ 30.96 \left( \frac{a}{w} \right) - 195.8 \left( \frac{a}{w} \right)^2 + 730.6 \left( \frac{a}{w} \right)^3 - 1186.3 \left( \frac{a}{w} \right)^4 + 754.6 \left( \frac{a}{w} \right)^5 \right]$$



The WOL specimen is shown in Figure 5. The crack opening is fixed by the bolt, and the loading is by constant displacement measured by means of a NASA type clip gage [3].

The cantilever beam method measures the crack extension threshold  $K_{I\text{ SCC}}$  whereas the (WOL) method measures the arrest value  $K_{I\text{ SCC}}$ . The crack initiation and propagation aspects can be best followed with the modified (WOL) specimen since the test can be periodically interrupted for microscopic examination without unloading the specimen. The final crack length is measured on the lateral faces of the specimen. The three dimensional aspects of the crack is determined by fracture of the sample and examination of the fracture surface. The effective crack length is determined by the relationship

$$a = \frac{a_L + a_m + a_R}{6}$$

Where  $a_m$  is the crack length at the middle of the specimen  $a_L$  and  $a_R$  are the crack lengths measured on the fracture surface on the left and right sides of the specimen respectively.

To determine changes in  $K_I$  with time as the crack propagates the crack length or can be measured periodically with a microscope and the force  $P$  and the stress intensity  $K_I$  may be calculated for any crack length  $a$  using the relationship

$$K_I = \frac{P_{C3} \left( \frac{a}{w} \right)}{(B B_N)^{1/2} a^{1/2}}$$

where  $B = 1$  for a 1T specimen and  $B_N$  is the actual value of the specimen thickness.

P(load is calculated from the equates

$$P = \frac{EB V_0}{C_6\left(\frac{a}{w}\right)}$$

where E is the modulus

B is specimen width

$V_0$  is the initial crack opening displacement

$C_6$  is a function of  $\left(\frac{a}{w}\right)$  obtain from compliance calibration data and give by

$$C_6\left(\frac{a}{w}\right) = e \left[ 3.453 - 8.097\left(\frac{a}{w}\right) + 42.314\left(\frac{a}{w}\right)^2 - 64.677\left(\frac{a}{w}\right)^3 + 36.845\left(\frac{a}{w}\right)^4 \right]$$